Supplementary Information

Stepwise Introduction of Dipole Blades into Triptycenes: Opening Variety of the Crystalline Molecular Packing Modes

Hikaru Yamamoto[1], Tsubakihara Yoshichika[2], Ayana-Sato-Tomita[3], Mingoo Jin[4]*

[1]Graduate School of Chemical Science and Engineering, Hokkaido University, Hokkaido 060-8628, Japan
[2]Department of Chemistry, Faculty of Science, Hokkaido University, Hokkaido 060-8628, Japan
[3]Division of Biophysics, Jichi Medical University, Tochigi, 329-0498, Japan
[4]Institute for Chemical Reaction Design and Discovery (WPI-ICReDD), Hokkaido University, Sapporo, Hokkaido, 060-8628, Japan

Email: mingoo@icredd.hokudai.ac.jp

Contents

1. General

All commercially available reagents and solvents are reagent grade and were used without further purification unless otherwise noted. Solvents for the synthesis were purchased from commercial suppliers, degassed by three freeze-pump-thaw cycles and further dried over molecular sieves (4 Å). NMR spectra were recorded on a JEOL JNM-ECX400P or JNM-ECS400 (^{1}H: 400 MHz; ^{13}C: 99.5 MHz) using tetramethylsilane and $CDCl_3$ as internal standards, respectively. Elemental analyses and low- and high-resolution mass spectra were recorded at the Global Facility Center at Hokkaido University.

2. Synthesis

2.1 Synthesis of 3b

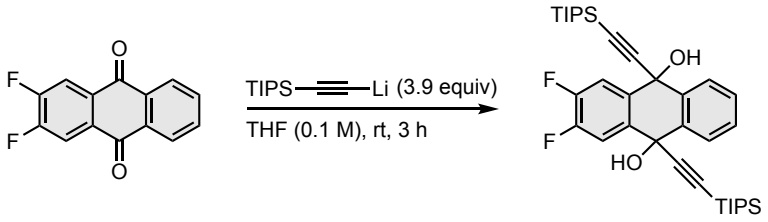

At –78 ºC, under a nitrogen atmosphere, *n*-BuLi in hexanes (1.55 M, 15.1 mL, 23.4 mmol) was added to a solution of TIPS-acetylene (5.38 mL, 4.38 g, 24.0 mmol) in THF (0.5 M). The mixture was allowed to stir for 15 min before being transferred slowly via cannula into a suspension of **2b** (1.5 g, 6.0 mmol) in THF (0.5 M). The resulting suspension was stirred for 3 h. After reaction, water was added, the organic layer was taken, and the aqueous phase extracted with CH_2Cl_2 (2 × 50 mL). The combined organic phases were dried $MgSO_4$ and taken to dryness under reduced pressure to give a solid residue. The crude material was purified by silica column using hexane/Et_2O (4:1) as an eluent provided the desired product **3b** (1.4 g, 38%). ^{1}H NMR (400 MHz, $CDCl_3$, δ): 1.04-1.10 (m, 42H), 2.89 (s, 2H), 7.48 (dd, *J* = 3.4 Hz and 5.8 Hz, 2H), 7.90 (t, *J* = 9.4 Hz, 2H), 8.06 (dd, *J* = 3.2 Hz and 5.6 Hz, 2H). ^{13}C NMR (100 MHz, $CDCl_3$, δ): ^{13}CNMR (100 MHz, $CDCl_3$, δ): 11.3 (*C*H), 18.6 (*C*H$_3$), 67.8 (*C*), 89.5 (*C*), 108.9 (C), 116.1 (dd, *J* = 7.1 Hz and 12.9 Hz, *C*H), 126.8 (*C*H), 129.3 (*C*H), 135.2 (t, *J* = 4.3 Hz, *C*), 137.5 (*C*), 150.5 (dd, *J* = 14.6 Hz and 249.9 Hz, *C*F). MS-EI (m/z): $[M+Cl]^+$ calcd for C36H50O2ClF2Si2, 643.30114; found, 643.30112.

2.2 Synthesis of 3c

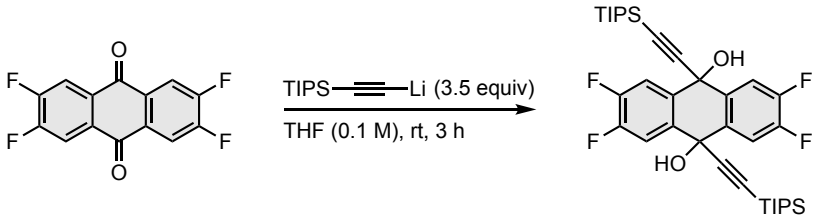

At –78 ºC, under a nitrogen atmosphere, *n*-BuLi in hexanes (1.55 M, 11.6 mL, 17.9 mmol) was added to a solution of TIPS-acetylene (4.13 mL, 3.36 g, 18.4 mmol) in THF (0.5 M). The mixture was allowed to stir for 15 min before being transferred slowly via cannula into a suspension of **2c** (1.3 g, 4.6 mmol) in THF (0.5 M). The resulting suspension was stirred for 3 h. After reaction, water was added, the

organic layer was taken, and the aqueous phase extracted with CH_2Cl_2 (2 × 50 mL). The combined organic phases were dried $MgSO_4$ and taken to dryness under reduced pressure to give a solid residue. The crude material was purified by silica column using hexane/Et_2O (4:1) as an eluent provided the desired product **3c** (1.6 g, 54%). ^{1}H NMR (400 MHz, $CDCl_3$, δ): 1.00-1.10 (m, 42H), 2.92 (s, 2H), 7.86 (t, *J* = 9.4 Hz, 4H). ^{13}C NMR (100 MHz, $CDCl_3$, δ): ^{13}CNMR (100 MHz, $CDCl_3$, δ): 11.2 (*C*H), 18.7 (*C*H$_3$), 67.3 (*C*), 90.5 (*C*), 108.0 (*C*), 116.2 (dd, *J* = 7.2 Hz and 12.8Hz, *C*H), 134.8 (t, *J* = 4.5 Hz, *C*), 150.6 (dd, *J* = 14.6 Hz and 250.6 Hz, *C*H). MS-EI (m/z): $[M+Cl]^+$ calcd for C36H48O2ClF4Si2, 679.28230; found, 679.28257.

2.3 Synthesis of 4b

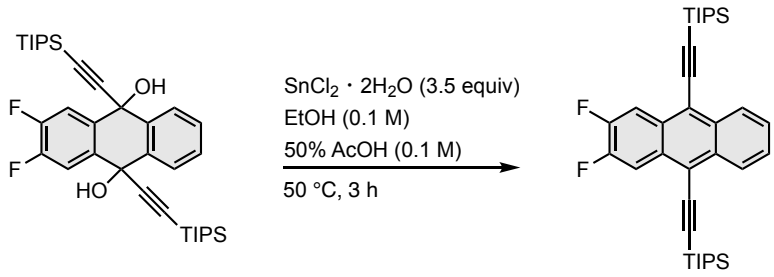

3b (1.4 g, 2.3 mmol) was dissolved in ethanol (0.1 M) in one-neck 200 mL flask and a solution of $SnCl_2 \cdot 2H_2O$ (2.8 g, 8.0 mmol) in 50% v/v AcOH aq. (0.1 M) was added dropwise. Once addition was complete, the suspension was stirred 50 ºC for 3 h. The reaction mixture was cooled to room temperature, and the precipitate was isolated by filtration washed with water and ethanol then dried thoroughly in vacuo. The crude material was purified by silica column using hexanes as an eluent provided the desired product **4b** (1.1 g, 82%). ^{1}H NMR (400 MHz, $CDCl_3$, δ): 1.23-1.35 (m, 42H), 7.61 (dd, *J* = 3.2 Hz and 6.8 Hz, 2H), 8.32 (t, *J* = 10.0 Hz, 2H), 8.57 (dd, *J* = 3.2 Hz and 6.8 Hz, 2H). ^{13}CNMR (100 MHz, $CDCl_3$, δ): 11.6 (*C*H), 19.0 (*C*H$_3$), 102.8 (*C*), 105.8 (*C*), 112.9 (dd, *J* = 6.2 Hz and 13.4 Hz, *C*H), 118.5 (*C*), 127.2 (*C*H), 127.4 (*C*H), 129.8 (t, *J* = 4.0 Hz, *C*), 132.5 (*C*), 151.3 (dd, *J* = 18.6 Hz and 253.5 Hz, *C*F). MS-EI (m/z): $[M+H]^+$ calcd for C36H49F2Si2, 575.33354; found, 575.33345.

2.4 Synthesis of 4c

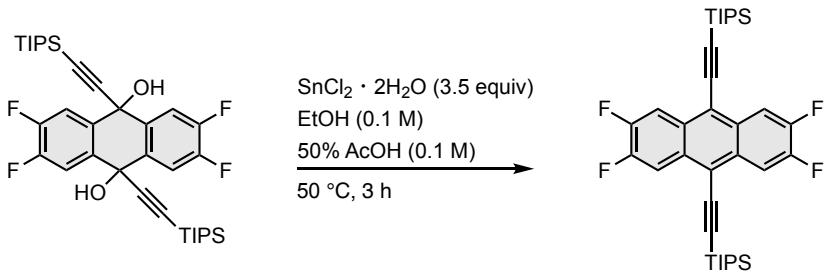

3c (1.6 g, 2.5 mmol) was dissolved in ethanol (0.1 M) in one-neck 200 mL flask and a solution of $SnCl_2 \cdot 2H_2O$ (3.0 g, 13 mmol) in 50% v/v AcOH aq. (0.1 M) was added dropwise. Once addition was complete, the suspension was stirred 50 ºC for 3 h. The reaction mixture was cooled to room temperature, and the precipitate was isolated by filtration washed with water and ethanol then dried thoroughly in vacuo. The crude material was purified by silica column using hexanes as an eluent provided the desired product **4c** (1.3 g, 83%). ^{1}H NMR (400 MHz, $CDCl_3$, δ): 1.23-1.54 (m, 42H), 8.26 (t, J = 9.8 Hz, 4H). ^{13}C NMR (100 MHz, $CDCl_3$, δ): 11.6 (*C*H), 19.0 (*C*H$_3$), 102.1 (C), 106.7 (*C*), 112.8-113.0 (m, *C*H), 118.0 (*C*), 129.8 (br, *C*), 151.6 (dd, d = 18.9 Hz and 254.7 Hz, *C*F). MS-EI (m/z): $[M+H]^+$ calcd for C36H46F4Si2, 611.31469; found, 611.31427.

2.5 Synthesis of 5b

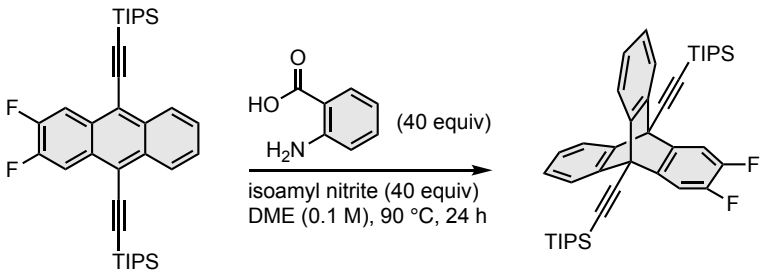

4b (1.48 g, 2.57 mmol) was dissolved in anhydrous 1,2-dimethoxyethane (130 mL) in a 3-neck flask equipped with two dropping funnels and condenser. The solution was heated to 100 °C and then a solution of anthranilic acid (14.3 g, 104 mmol) and iso-amyl nitrite (12.3 g, 13.8 mL, 104 mmol) in anhydrous 1,2-dimethoxyethane (65 mL) were slowly added via additional funnels over a period of 1.5 h. The reaction mixture was heated to 90 °C for additional 24 h before being cooled to room temperature. The solvent was removed under reduced pressure, and the residue was purified by silica gel column chromatography (hexane as eluent) to afford **5b** (0.69 g, 41% yield). ^{1}H NMR (400 MHz,

$CDCl_3$, δ): 1.23-1.39 (m, 42H), 7.12 (dd, *J* = 3.2 Hz and 5.6 Hz, 4H), 7.55 (t, *J* = 8.6 Hz, 2H), 7.74 (dd, *J* = 3.4 Hz and 5.4 Hz, 4H). ^{13}C NMR (100 MHz, $CDCl_3$, δ): 11.6 (*C*H), 19.0 (*C*H_3), 53.0 (*C*), 94.9 (*C*), 100.7 (*C*), 112.6 (dd, *J* = 7.6 Hz, 13.4 Hz, *C*H), 122.5 (*C*H), 126.2 (*C*H), 140.6 (t, *J* = 4.3 Hz, *C*), 143.3 (*C*), 148.1 (dd, *J* = 14.8 Hz and 246.8 Hz, *C*F). MS-EI (m/z): $[M+H]^+$ calcd for C42H53F2Si2, 651.36484; found, 651.36479.

2.6 Synthesis of 5c

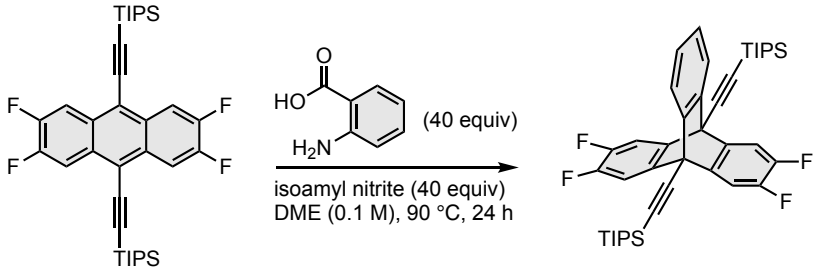

4c (1.8 g, 3.0 mmol) was dissolved in anhydrous 1,2-dimethoxyethane (150 mL) in a 3-neck flask equipped with two dropping funnels and condenser. The solution was heated to 100 °C and then a solution of anthranilic acid (16.5 g, 120 mmol) and iso-amyl nitrite (14.0 g, 16.0 mL, 120 mmol) in anhydrous 1,2-dimethoxyethane (75 mL) were slowly added via additional funnels over a period of 1.5 h. The reaction mixture was heated to 90 °C for additional 24 h before being cooled to room temperature. The solvent was removed under reduced pressure, and the residue was purified by silica gel column chromatography (hexane as eluent) to afford **5b** (0.30 g, 14% yield). ^{1}H NMR (400 MHz, $CDCl_3$, δ): 1.26-1.37 (m, 42H), 7.15 (dd, *J* = 3.2 Hz and 5.6 Hz, 2H), 7.53 (t, *J* = 8.4 Hz, 4H), 7.72 (dd, *J* = 3.2 Hz and 5.6 Hz, 2H). ^{13}C NMR (100 MHz, $CDCl_3$, δ): 11.5 (*C*H), 19.0 (*C*H_3), 52.5 (*C*), 95.5 (*C*), 99.8 (*C*), 112.7 (dd, *J* = 7.6 Hz, 13.4 Hz, *C*H), 122.5 (*C*H), 126.5 (*C*H), 140.0 (t, *J* = 4.5 Hz, *C*), 142.7 (*C*), 148.1 (dd, *J* = 14.6 Hz and 247.5 Hz, *C*F). MS-EI (m/z): $[M]^+$ calcd for C42H50F4Si2, 686.33817; found, 686.33802.

2.7 Synthesis of 1b

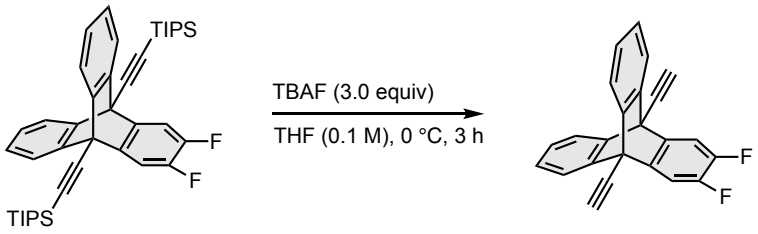

5b (2.06 g, 3.17 mmol) was dissolved in anhydrous THF (0.1 M) at 0 °C and TBAF (1.0 M solution in THF, 9.5 mL) was added dropwise. The reaction mixture was stirred in an ice bath at 0 °C for 3 h, and then quenched by the additional of saturated NH_4Cl solution. The product was extracted with CH_2Cl_2 (3×30 mL). The combined organic layers were dried over anhydrous $MgSO_4$ and concentrated under reduced pressure to afford a pale-orange residue. Purification by silica gel column chromatography (hexane as eluent) gave **1b** (0.61 g, 57%). ^{1}H NMR (400 MHz, $CDCl_3$, δ): 3.31 (s, 2H), 7.14 (dd, *J* = 3.2 and 5.6 Hz, 4H), 7.57 (t, *J* = 8.8 Hz, 2H), 7.74 (dd, *J* = 3.2 Hz and 5.6 Hz, 4H). ^{13}C NMR (100 MHz, $CDCl_3$, δ): 51.8 (*C*), 77.5 (*C*H), 81.4 (*C*), 112.5 (dd, *J* = 7.7 Hz and 13.3 Hz, *C*H), 122.4 (*C*H), 126.3 (*C*H), 139.9 (t, *J* = 4.5 Hz, *C*), 148.1 (dd, *J* = 14.6 Hz and 247.0 Hz). MS-EI (m/z): $[M]^+$ calcd for C24H12F2, 338.09016; found, 338.09003. Element analysis (calcd for C24H12F2 C, 85.20; H, 3.57; Found: C, 85.20; H, 3.57).

2.8 Synthesis of 1c

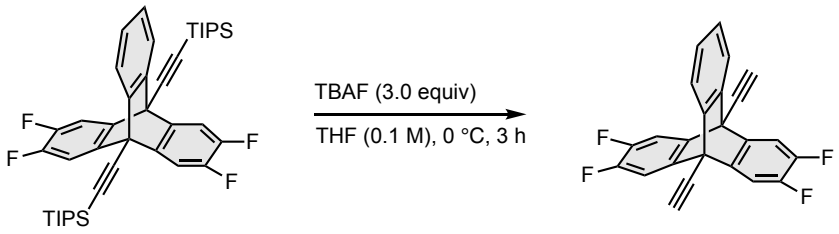

5c (0.30 g, 0.43 mmol) was dissolved in anhydrous THF (0.1 M) at 0 °C and TBAF (1.0 M solution in THF, 1.3 mL) was added dropwise. The reaction mixture was stirred in an ice bath at 0 °C for 3 h, and then quenched by the additional of saturated NH_4Cl solution. The product was extracted with CH_2Cl_2 (3×30 mL). The combined organic layers were dried over anhydrous $MgSO_4$ and concentrated under reduced pressure to afford a pale-orange residue. Purification by silica gel column chromatography (hexane as eluent) gave **1c** (0.61 g, 43%). ^{1}H NMR (400 MHz, $CDCl_3$, δ): 3.34 (s, 2H), 7.16 (dd, *J* = 3.2 and 5.6 Hz, 2H), 7.55 (t, *J* = 8.6 Hz, 4H), 7.72 (dd, *J* = 3.2 Hz and 5.6 Hz, 2H). ^{13}C NMR (100 MHz, $CDCl_3$, δ): 51.2 (*C*), 76.8 (*C*H), 81.8 (*C*), 112.6 (dd, *J* = 7.6 Hz and 13.4 Hz, *C*H), 122.5 (*C*H),

126.6 (*C*H), 139.3 (t, *J* = 4.8 Hz, *C*), 148.2 (dd, *J* = 14.5 Hz and 248.1 Hz). MS-EI (m/z): $[M]^+$ calcd for C24H10F4, 374.07131; found, 374.07116. Element analysis (calcd for C24H10F4 C, 85.20; H, 3.57; Found: C, 85.35; H, 3.94).

3. Thermogravimetric Analysis (TGA) of Crystals 1a, 1b and 1c

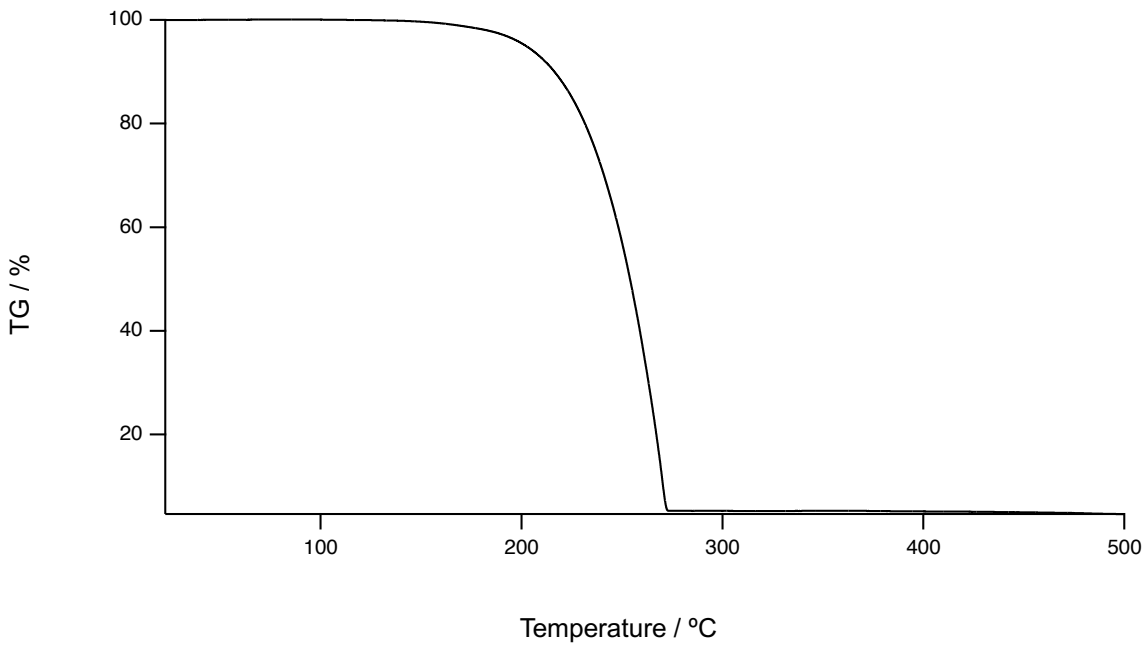

Fig. S1. TGA profiles of the crystal **1a**. The heating rate is 5 °C/min.

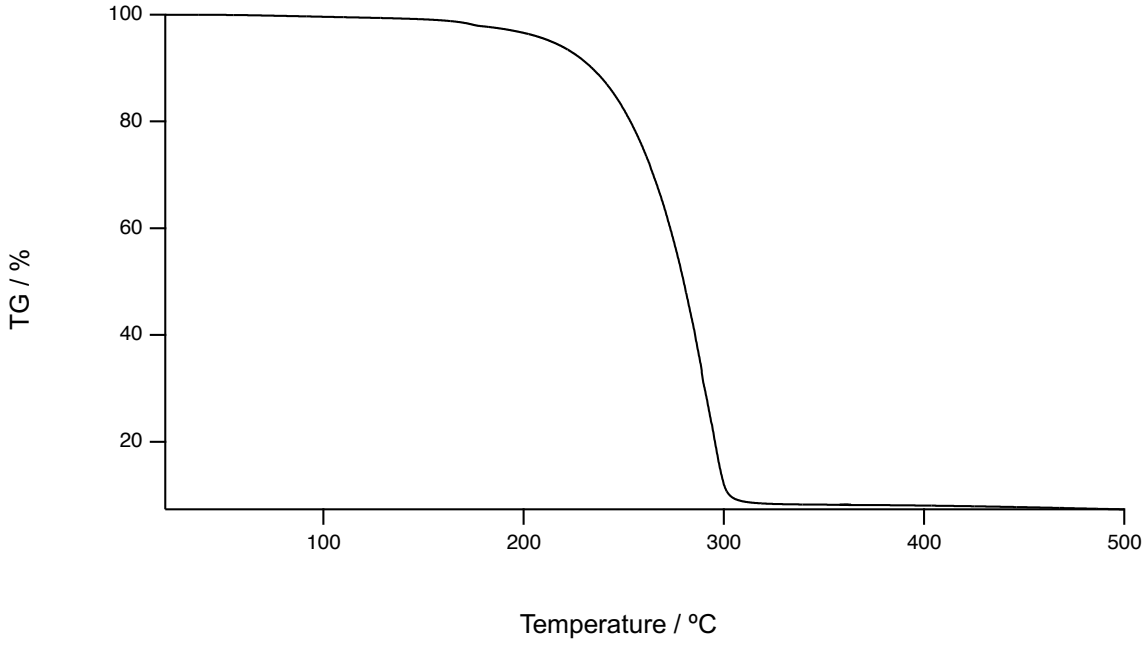

Fig. S2. TGA profiles of the crystal **1b**. The heating rate is 5 °C/min.

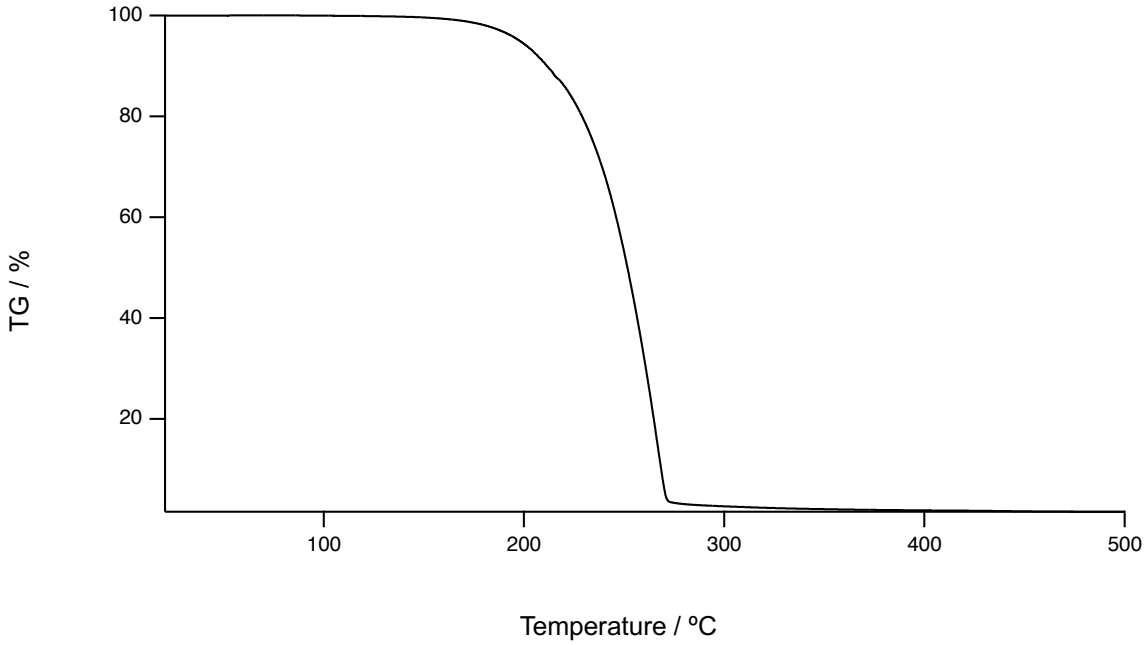

Fig. S3. TGA profiles of the crystal **1c**. The heating rate is 5 °C/min.

4. Differential Scanning Calorimetry (DSC) of Crystal 1a, 1b and 1c

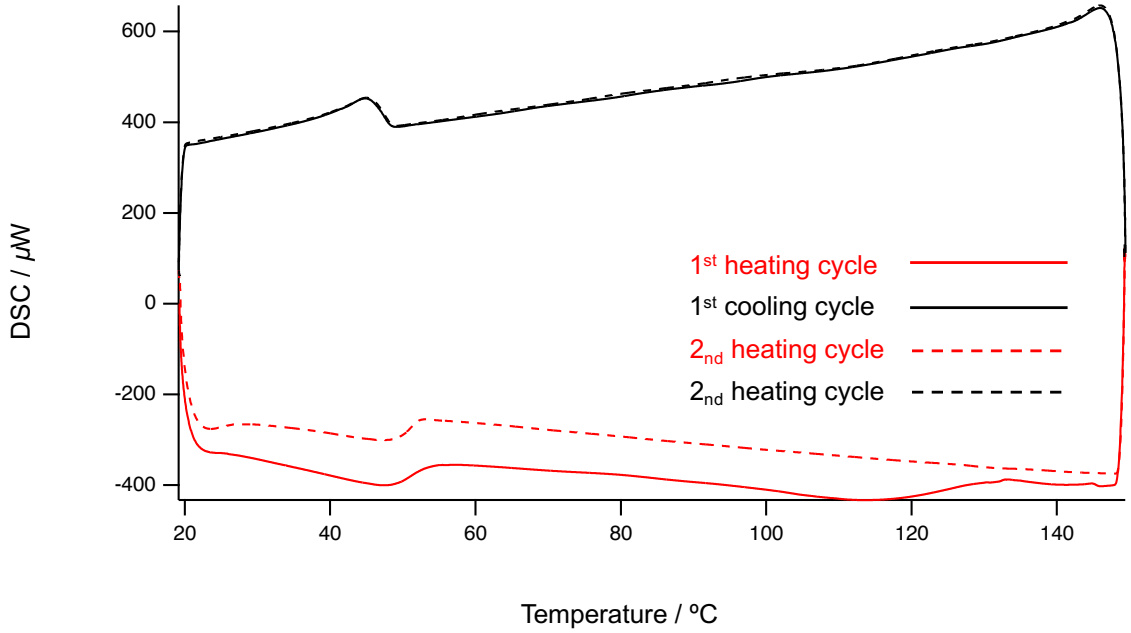

Fig. S4. DSC profiles of the crystal **1a**. Heating and cooling rates were 5 °C/min.

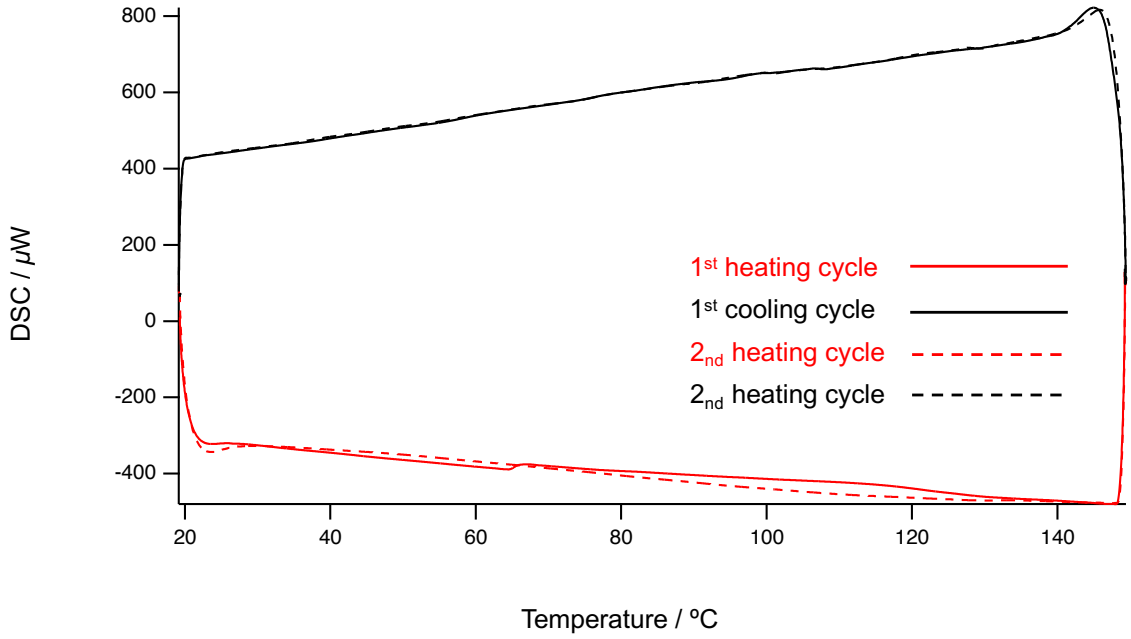

Fig. S5. DSC profiles of the crystal **1b**. Heating and cooling rates were 5 °C/min.

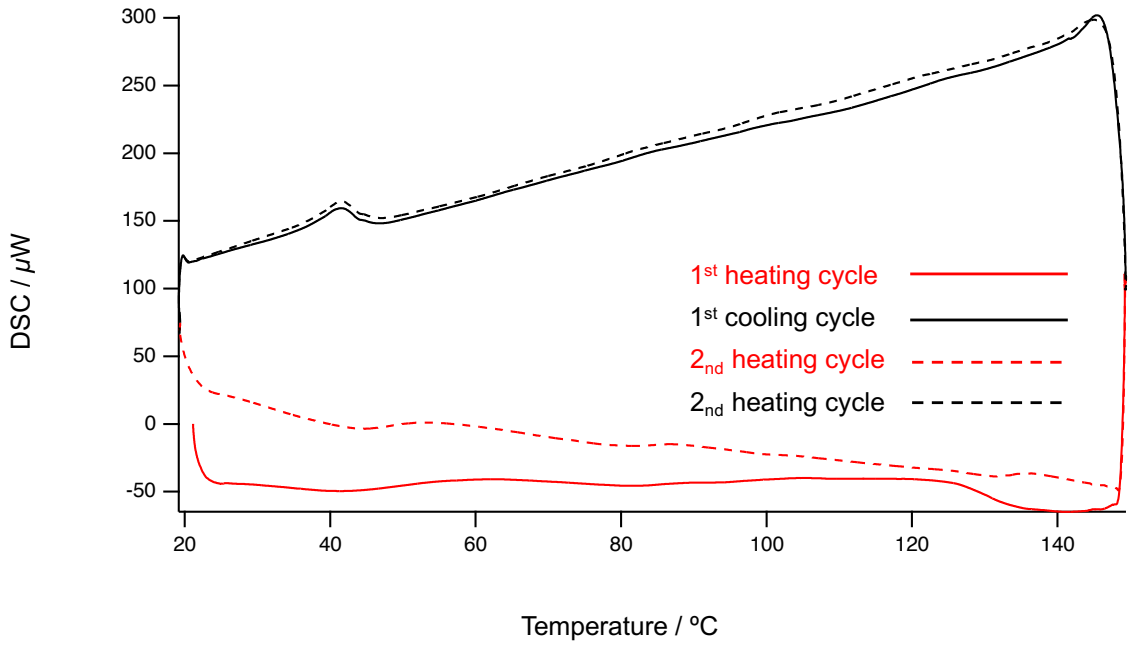

Fig. S6. DSC profiles of the crystal **1c**. Heating and cooling rates were 5 °C/min.

5. Single-Crystal X-Ray Structural Analyses

Single-crystal X-ray structural analyses were carried out on a Rigaku XtaLAB PRO MM007 diffractometer using graphite monochromated Cu-K_α radiation. The structures were solved using intrinsic phasing as implemented in the SHELXT program and refined by full-matrix least-squares on F^2 using SHELXL within the OLEX2 program package.[2] Non-hydrogen atoms were refined anisotropically. Hydrogen atoms were refined using the riding model.

compound	**1a**	**1b**	**1c (*P*4$_1$)**	**1c (*P*4$_3$)**
CCDC Number	2493853	2493852	2493850	2493851
Empirical Formula	$C_{24}H_{14}$	$C_{24}H_{12}F_2$	$C_{24}H_{10}F_4$	$C_{24}H_{10}F_4$
Formula Weight	302.35	338.34	374.32	374.32
Crystal System	monoclinic	monoclinic	tetragonal	tetragonal
Crystal Size / mm	0.05×0.05×0.05	0.05×0.05×0.05	0.05×0.05×0.05	0.01×0.01×0.01
a / Å	8.11040(1)	8.20240(1)	13.4142(6)	13.5057(5)
b / Å	27.2387(3)	32.5749(3)	13.4142(6)	13.5057(5)
c / Å	8.34000(1)	13.25110(1)	9.5889(7)	9.6580(6)
α / °	90	90	90	90
β / °	116.276(2)	101.794(1)	90	90
γ / °	90	90	90	90
V / Å^3	1652.07(4)	3465.85(6)	1725.4(2)	1761.66(17)
Space Group	*Cc*	*P*21/*c*	*P*4$_1$	*P*4$_3$
Z value	4	8	4	4
D_{calc} / g cm^{-3}	1.216	1.297	1.441	1.411
Temperature / K	293	293	153	293
$2\theta_{max}$ / °	151.276	68.56	155.938	149.406
μ / mm^{-1}	0.525	0.100	0.964	0.944
No. of Reflections	Total: 15033	Total: 31556	Total: 16038	Total: 8939
	Unique:2997	Unique:10742	Unique:3500	Unique:3435
	R_{int} = 0.0231	R_{int} = 0.0566	R_{int} = 0.0609	R_{int} = 0.0371
R_1[a]	0.0285	0.0624	0.0524	0.0522
wR_2[b]	0.0783	0.1845	0.1341	0.1642
GOF[c]	1.073	1.040	1.071	1.091
Flack Parameter	-0.2(5)		-0.06(15)	-0.1(3)
Max./Mini. peak *I*[d] / Å	0.13 e$^-$/-0.11 e$^-$	0.35 e$^-$/-0.30 e$^-$	0.24 e$^-$/−0.27 e$^-$	0.18 e$^-$/−0.15 e$^-$

[a]: $I > 2.00\sigma(I)$. [b]: All reflections. [c]: Goodness of Fit Indicator.

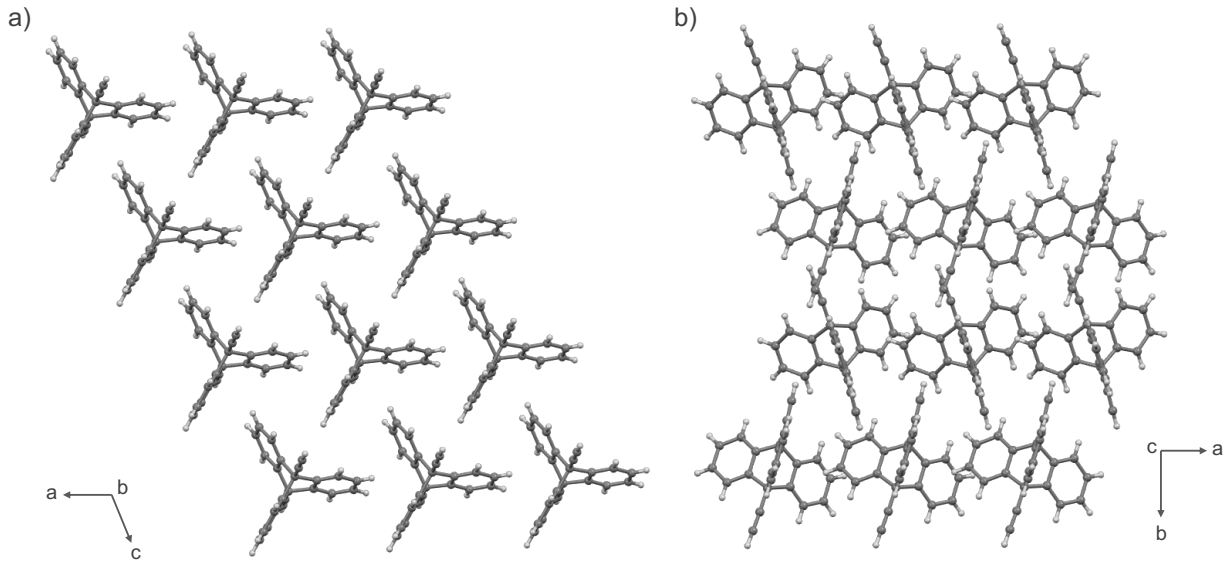

Figure S7. Crystal structure of **1a**. a) The two-dimensional intermeshed structure extending along the *ac* plane. b) The intermeshed layers stack in a zigzag fashion along the *b* direction.

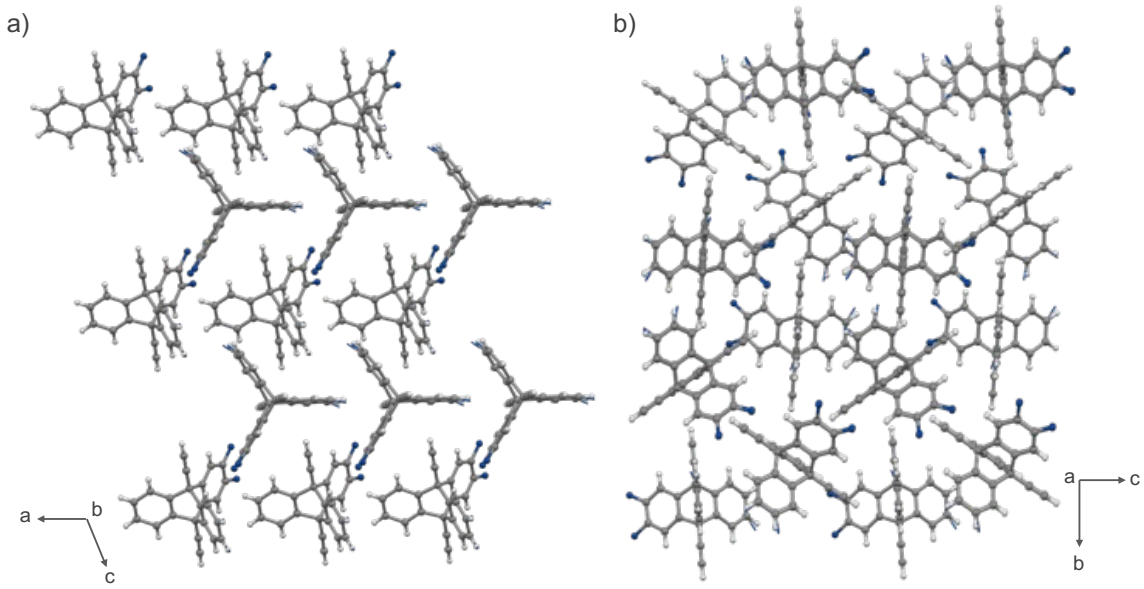

Figure S8. Crystal structure of **1b**. a) The one-dimensional intermeshed structure extending along the *ac* plane. b) The intermeshed layers stack along the *b* direction.

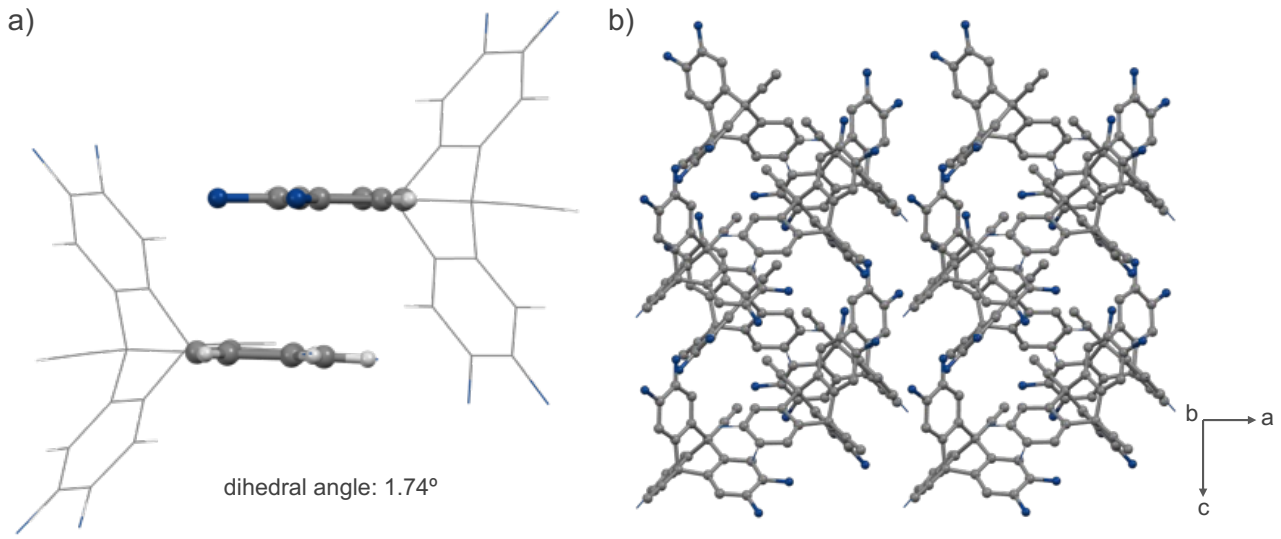

Figure S9. Crystal structure of **1c** ($P4_1$). a) π–π stacking interaction between the phenylene and fluoro-phenylene units, showing the dihedral angle between their aromatic planes. b) Packing structure between the helical columns of **1c** ($P4_1$). Adjacent columns possess the same helical handedness, and thus the molecular dipoles are not canceled out.

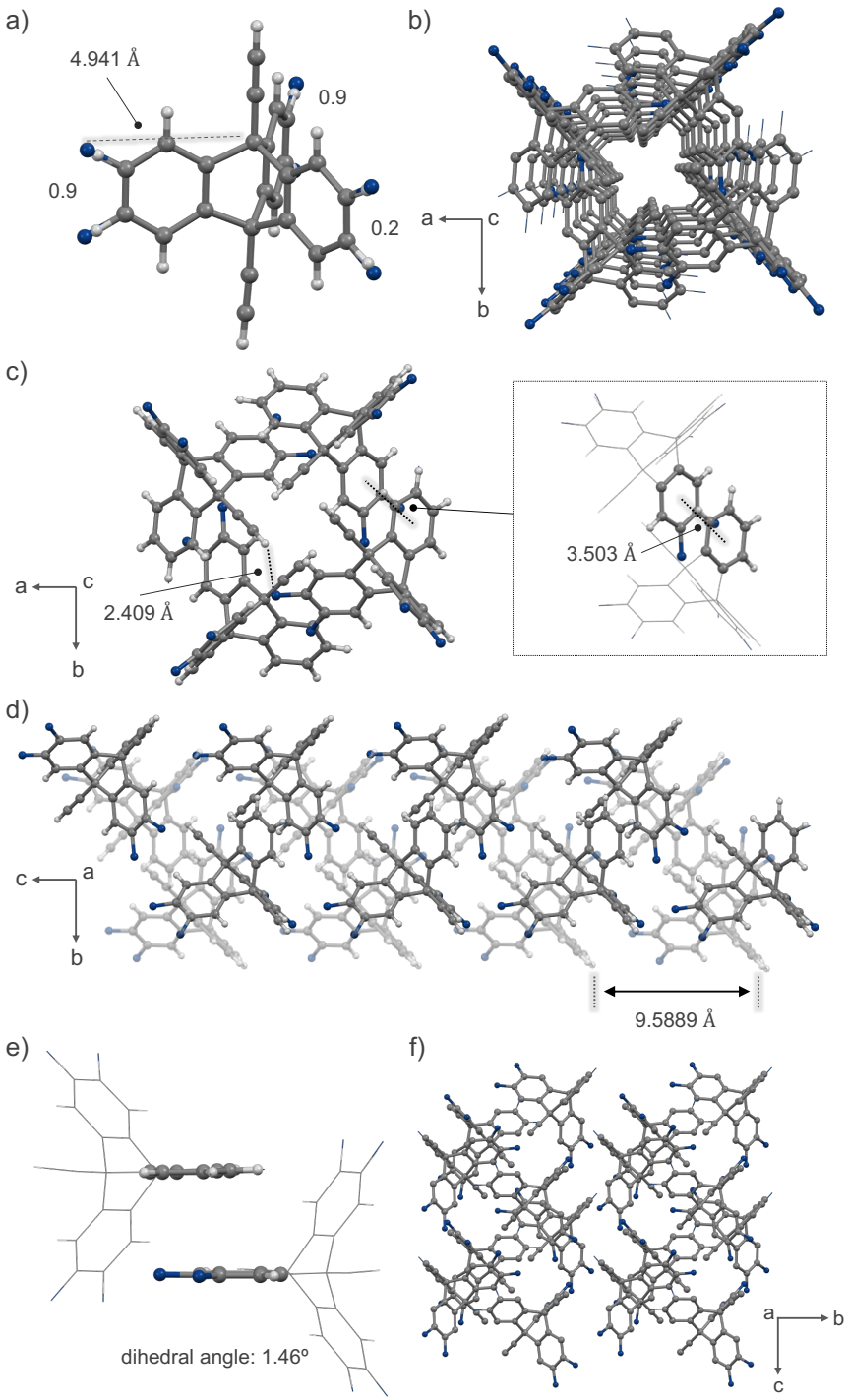

Figure S10. Crystal structure of **1c** ($P4_3$). (a) monomer structure. (b) top view and (c) side view of P-helicity of the 4-fold helical structure; (d) observed π-π interaction and H···F close contact. e) π–π stacking interaction between the phenylene and fluoro-phenylene units, showing the dihedral angle between their aromatic planes. f) Packing structure between the helical columns of **1c** ($P4_3$). Adjacent columns possess the same helical handedness, and thus the molecular dipoles are not canceled out.

6. DFT calculations

All the calculations were performed at the DFT level of theory with the B3LYP hybrid functional[3] as implemented in Gaussian 16.[4] To describe the dispersion properly, the D3 version of Grimme's dispersion with the Becke-Johnson damping[5] was employed in the DFT calculations. The Pople-style 6-311+G(d,p) basis sets were used for the geometry optimization.[6] The geometries of the tetramers were taken from the single crystal structures of **1a**, **1b**, and **1c**.

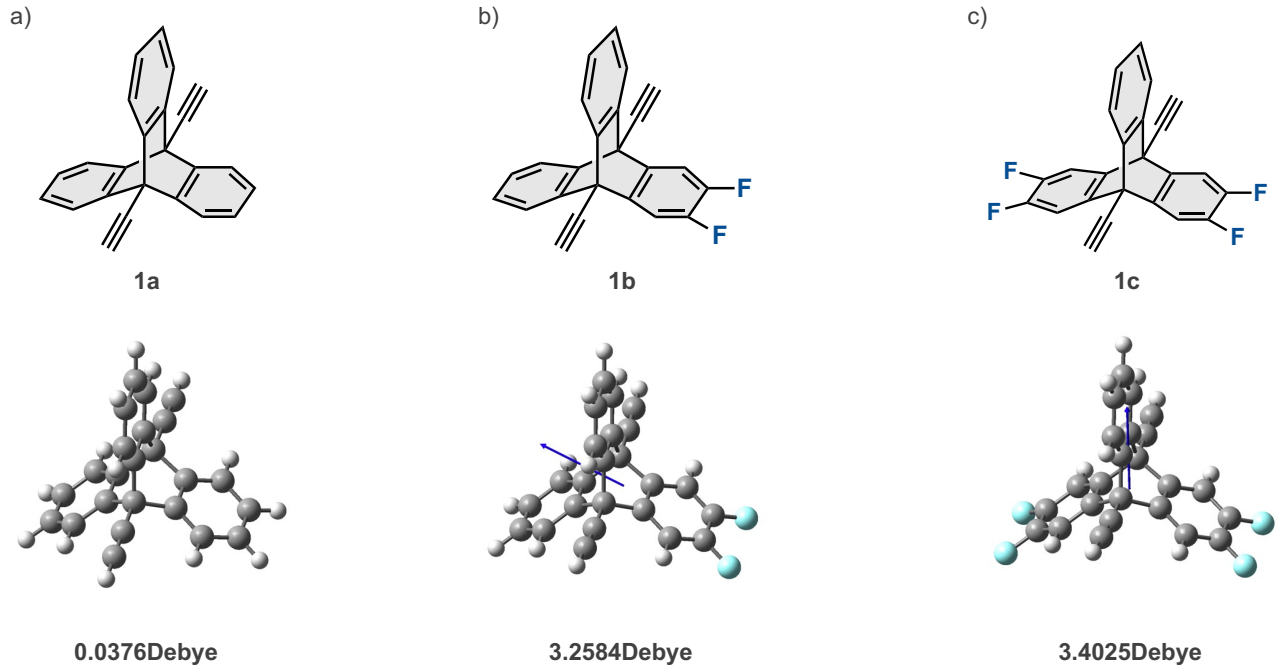

Figure S11. The dipole moments of the monomers **1a**, **1b**, and **1c**. Blue arrows indicate the dipole moment vectors obtained from DFT calculations, with the corresponding magnitudes shown in debye.

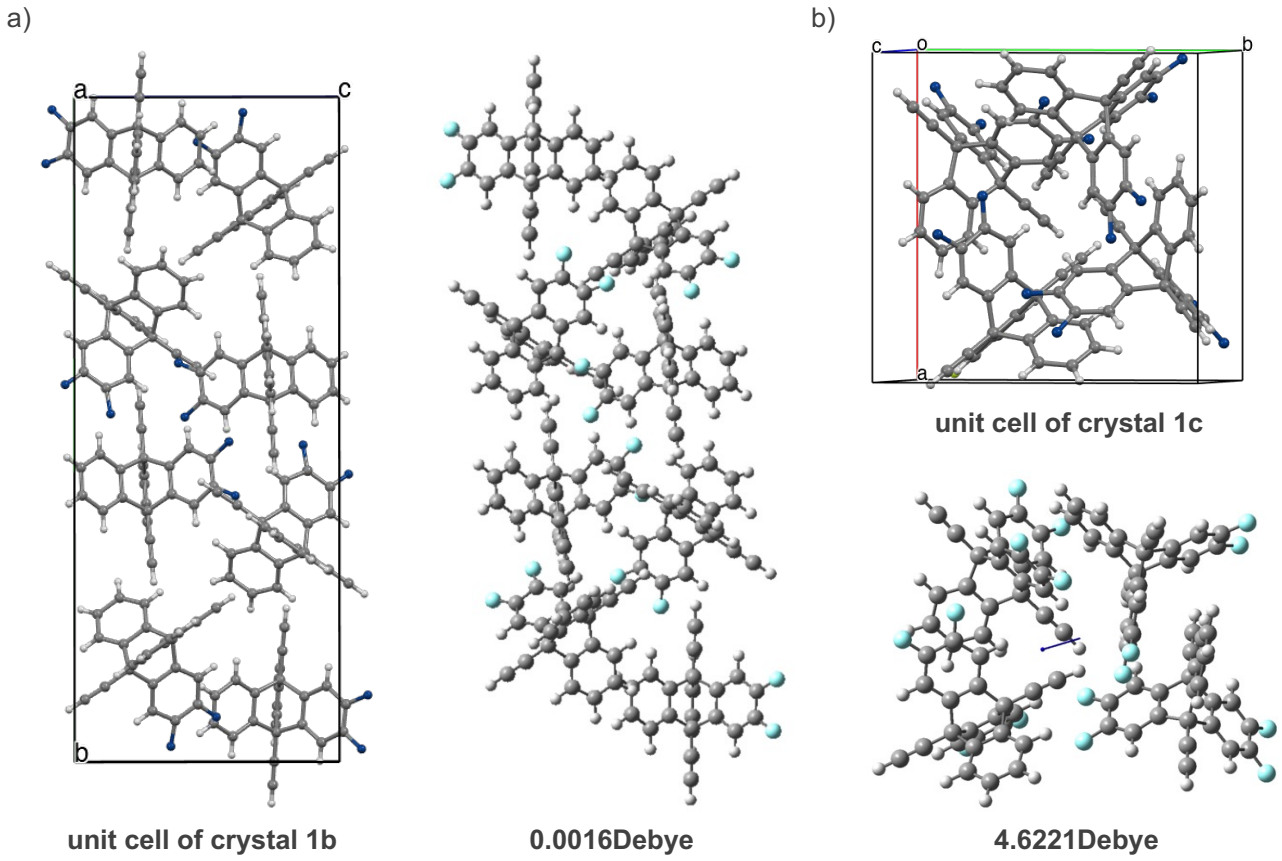

Figure S12. The dipole moments of the unit cells **1b**, and **1c**. Blue arrows indicate the dipole moment vectors obtained from DFT calculations, with the corresponding magnitudes shown in debye. Although monomer **1b** possesses a distinct dipole moment, the overall dipole moment cancels out in the crystal unit cell due to its symmetric packing arrangement.

7. Analysis of Non-Covalent Interactions of Crystal 1b and 1c

Independent Gradient Model based on Hirshfeld partition (IGMH) analysis of the crystal structures of **1b** and **1c**, performed using the experimental single-crystal X-ray diffraction geometries of their unit cells.[7] For **1b**, no pronounced localized non-covalent interactions are observed, indicating that its crystal packing is not governed by specific directional intermolecular interactions and is instead dominated by isotropic dispersion forces. In contrast, the IGMH analysis of **1c** reveals distinct non-covalent interaction regions corresponding to π–π stacking and C≡C–H···F hydrogen bonding, suggesting that these directional interactions cooperatively contribute to the stabilization of the polar helical packing structure.

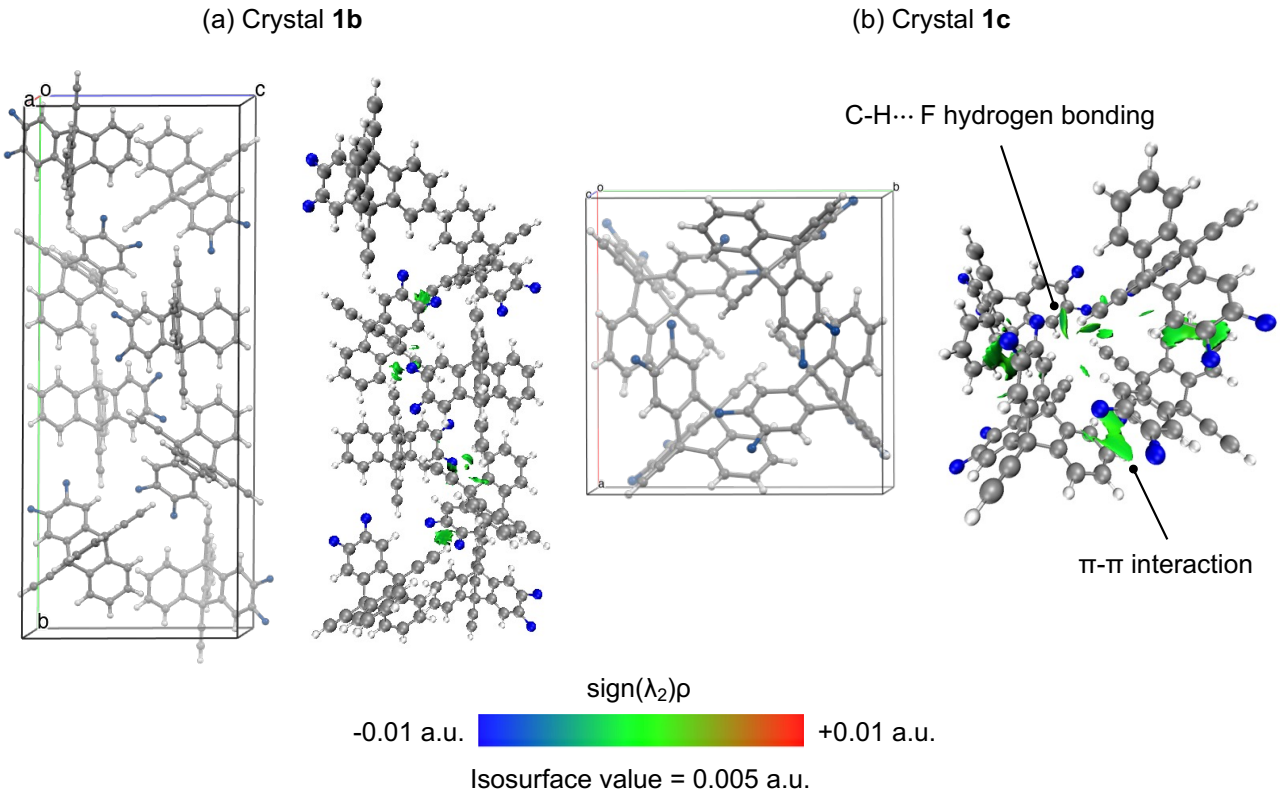

Figure S13. Visualization of IGMH analysis (sign(λ_2)ρ colored isosurfaces of δg_{inter}) of unit cell in the crystal structures of (a)**1b** and (b)**1c**.

8. Reference

1 O. V. Dolomanov, L. J. Bourhis, R. J. Gildea, J. A. K. Howard and H. Puschmann, *J. Appl. Crystallogr.*, 2009, **42**, 339–341.

2 G. M. Sheldrick, *Acta Crystallogr. C Struct. Chem.*, 2015, **71**, 3–8.

3 (a) A. D. Becke, J. Chem. Phys., 1993, **98**, 1372–1377. (b) C. Lee, W. Yang and R. G. Parr, *Phys. Rev. B Condens. Matter*, 1988, **37**, 785–789.

4 Gaussian 16, Revision C.01, M. J. Frisch, G. W. Trucks, H. B. Schlegel, G. E. Scuseria, M. A. Robb, J. R. Cheeseman, G. Scalmani, V. Barone, G. A. Petersson, H. Nakatsuji, X. Li, M. Caricato, A. V. Marenich, J. Bloino, B. G. Janesko, R. Gomperts, B. Mennucci, H. P. Hratchian, J. V. Ortiz, A. F. Izmaylov, J. L. Sonnenberg, D. Williams-Young, F. Ding, F. Lipparini, F. Egidi, J. Goings, B. Peng, A. Petrone, T. Henderson, D. Ranasinghe, V. G. Zakrzewski, J. Gao, N. Rega, G. Zheng, W. Liang, M. Hada, M. Ehara, K. Toyota, R. Fukuda, J. Hasegawa, M. Ishida, T. Nakajima, Y. Honda, O. Kitao, H. Nakai, T. Vreven, K. Throssell, J. A. Montgomery Jr., J. E. Peralta, F. Ogliaro, M. J. Bearpark, J. J. Heyd, E. N. Brothers, K. N. Kudin, V. N. Staroverov, T. A. Keith, R. Kobayashi, J. Normand, K. Raghavachari, A. P. Rendell, J. C. Burant, S. S. Iyengar, J. Tomasi, M. Cossi, J. M. Millam, M. Klene, C. Adamo, R. Cammi, J. W. Ochterski, R. L. Martin, K. Morokuma, O. Farkas, J. B. Foresman and D. J. Fox, *Gaussian, Inc.*, Wallingford CT, 2016.

5 (a) S. Grimme, J. Antony, S. Ehrlich and H. Krieg, *J. Chem. Phys.*, 2010, **132**, 154104. (b) S. Grimme, S. Ehrlich and L. Goerigk, *J. Comput. Chem.*, 2011, **32**, 1456–1465.

6 (a) A. D. McLean and G. S. Chandler, *J. Chem. Phys.*, 1980, **72**, 5639–5648. (b) R. Krishnan, J. S. Binkley, R. Seeger and J. A. Pople, *J. Chem. Phys.*, 1980, **72**, 650–654.

7 T. Lu and Q. Chen, *J. Comput. Chem.*, 2022, **43**, 539–555.

9. NMR spectra

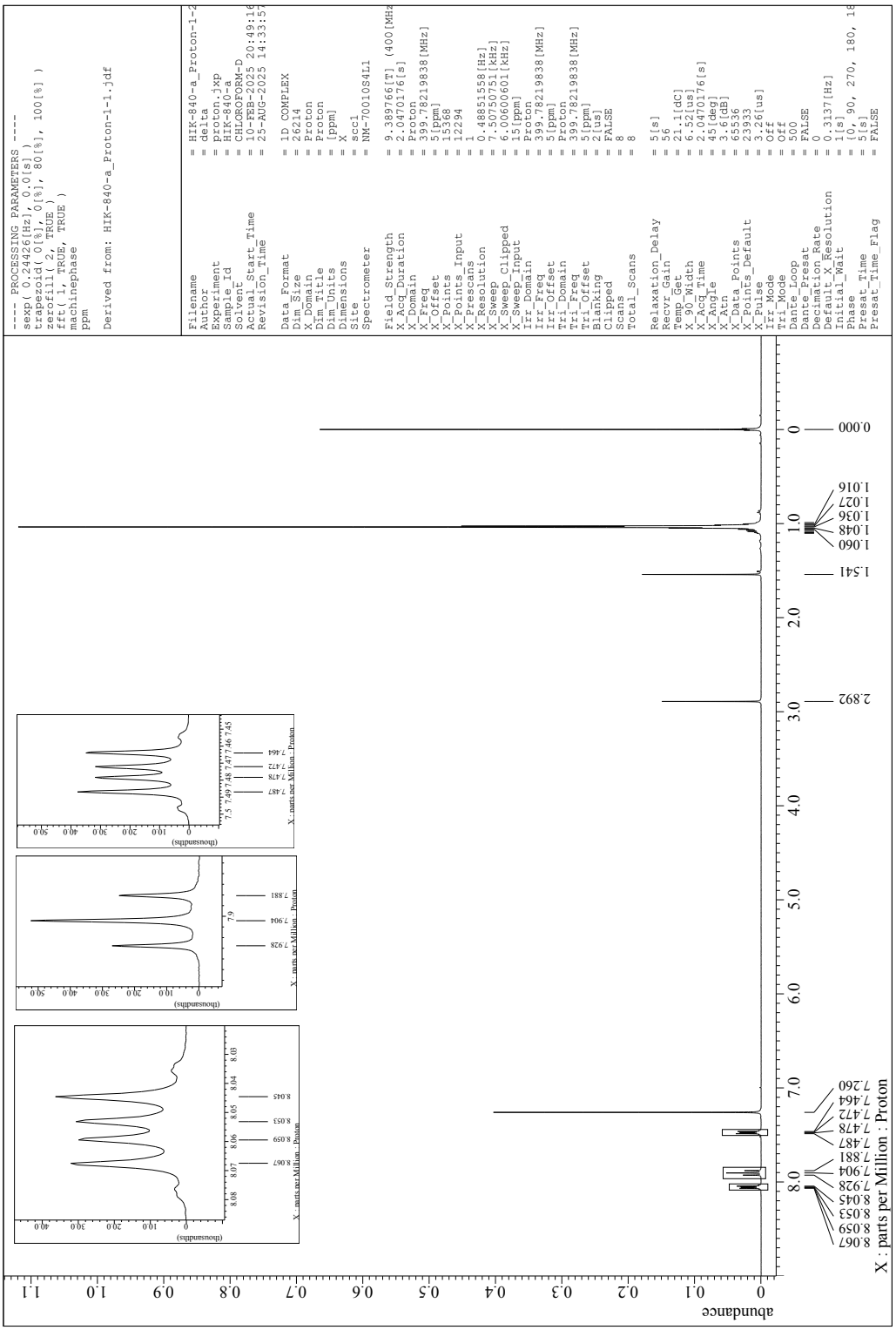

Figure S14. ^{1}H NMR spectrum (400 MHz, $CHCl_3$) of **3b**

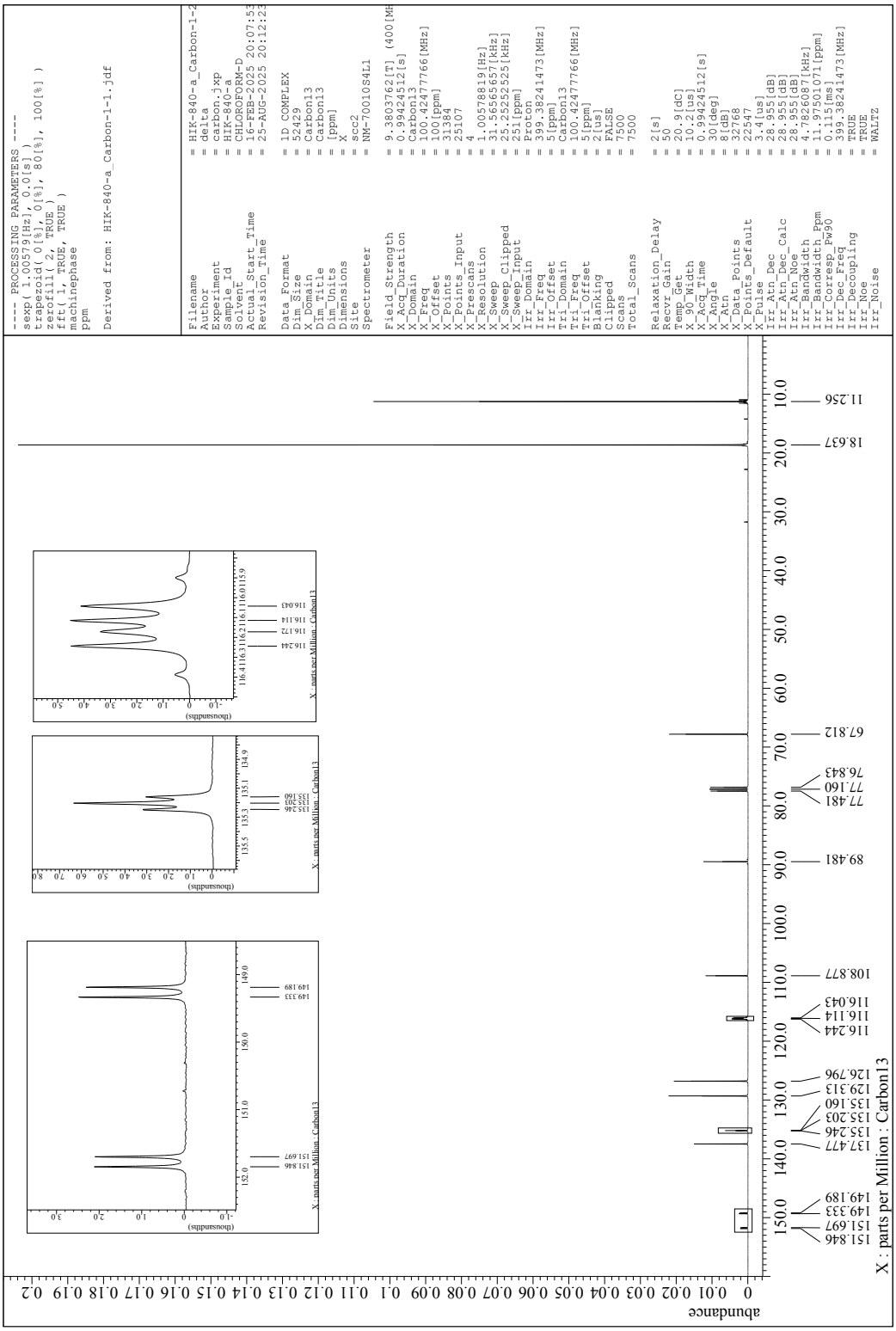

Figure S15. ^{13}C NMR spectrum (100 MHz, $CHCl_3$) of **3b**

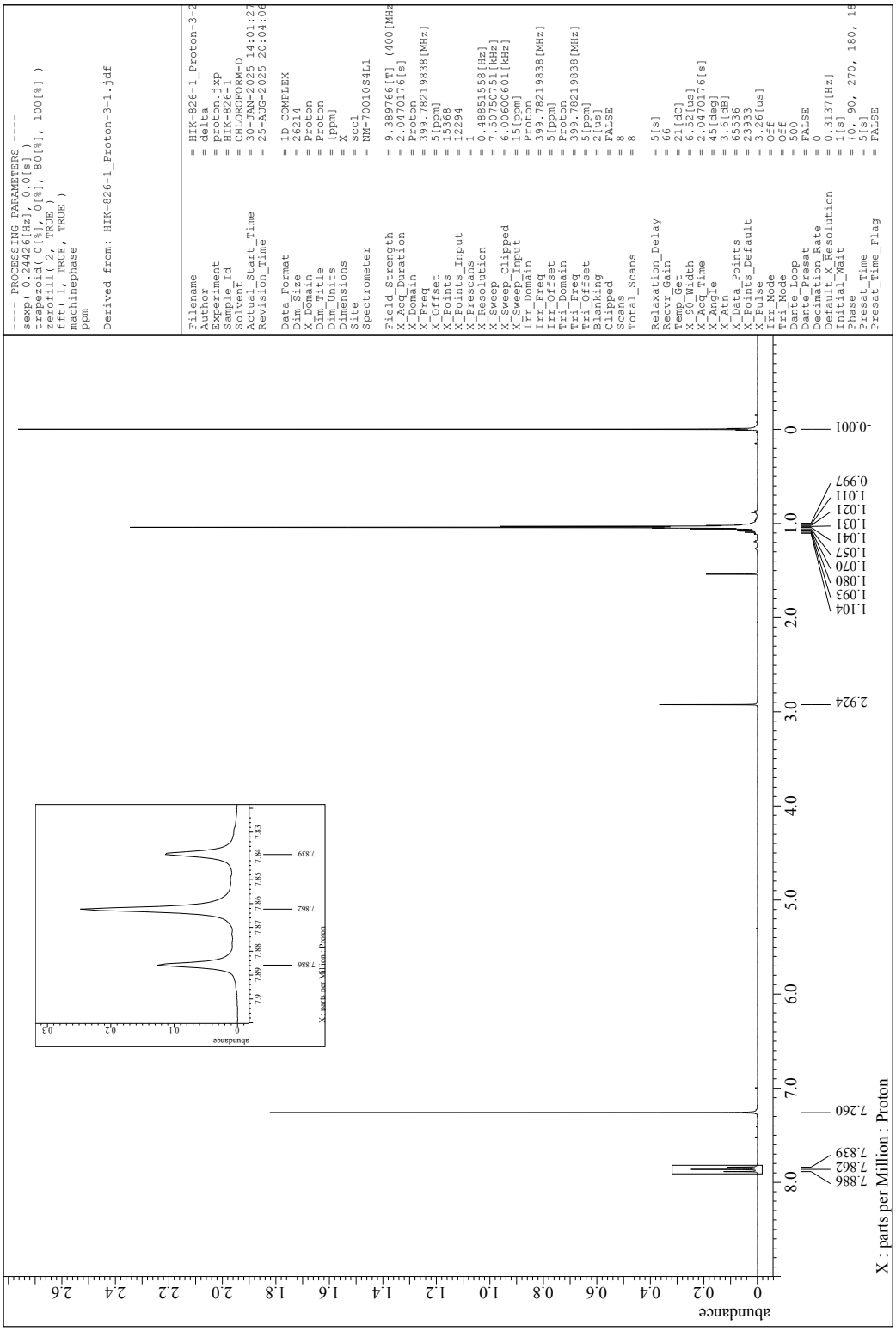

Figure S16. ^{1}H NMR spectrum (400 MHz, $CHCl_3$) of **3c**

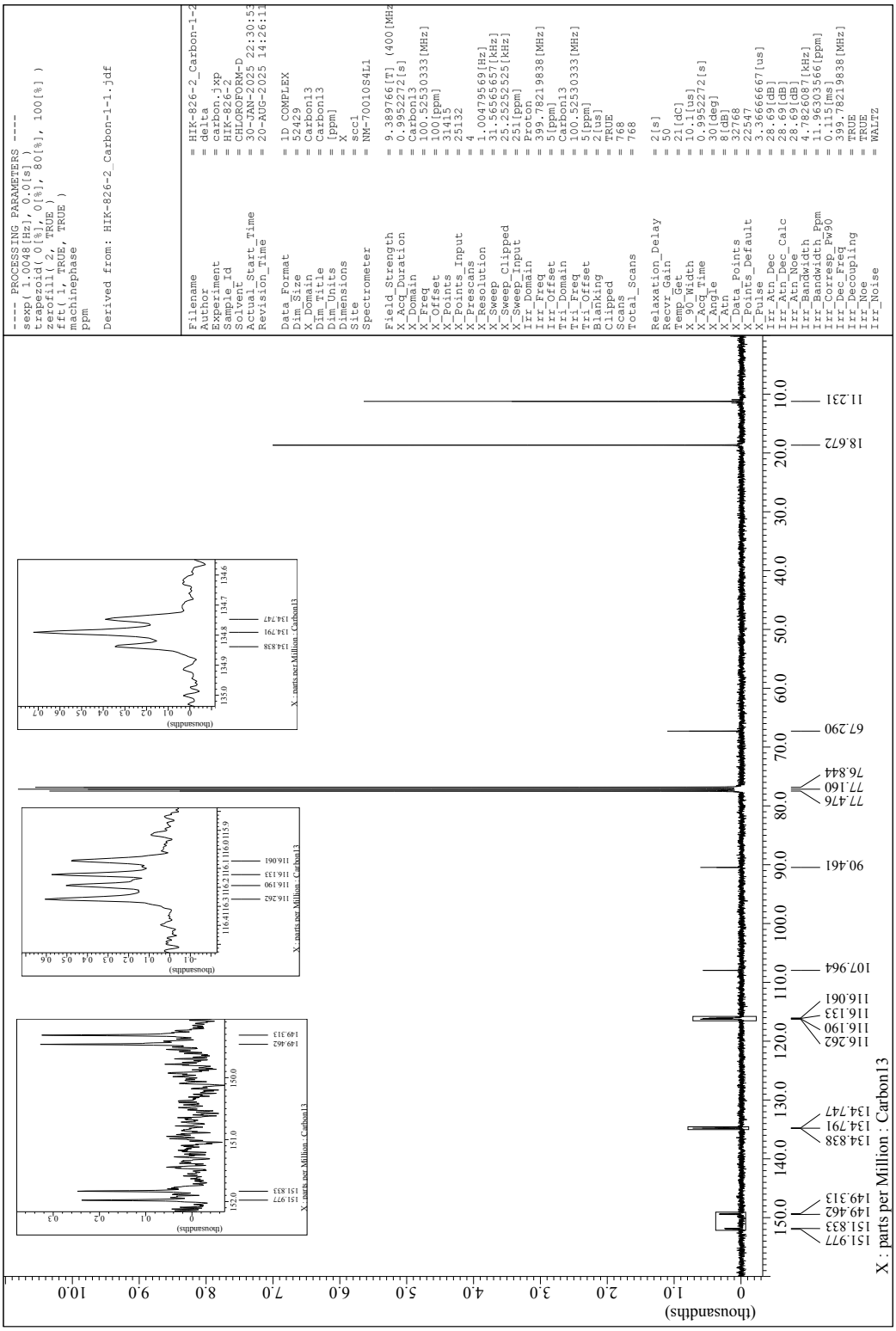

Figure S17. ^{13}C NMR spectrum (100 MHz, $CHCl_3$) of **3c**

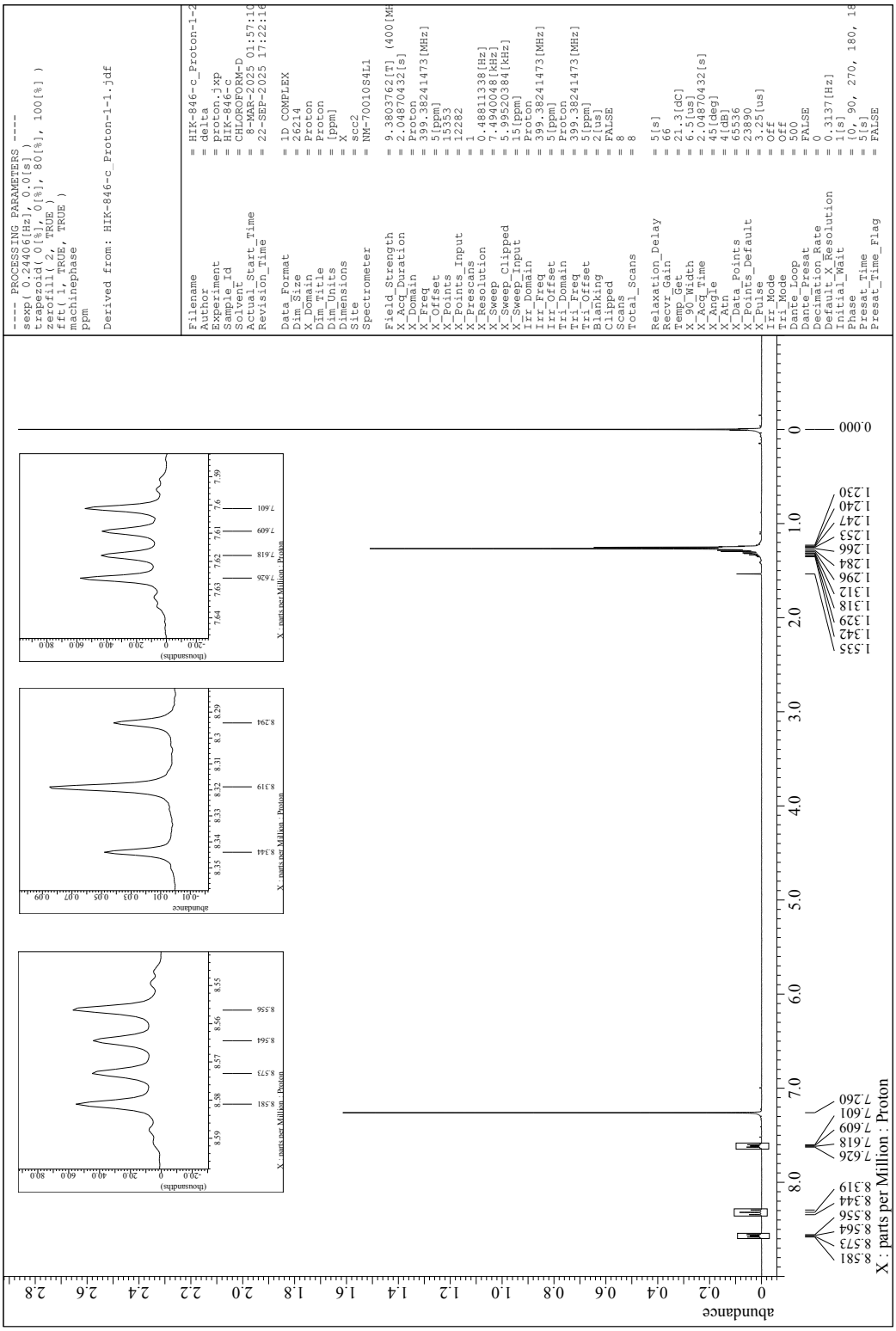

Figure S18. ^{1}H NMR spectrum (400 MHz, $CHCl_3$) of **4b**

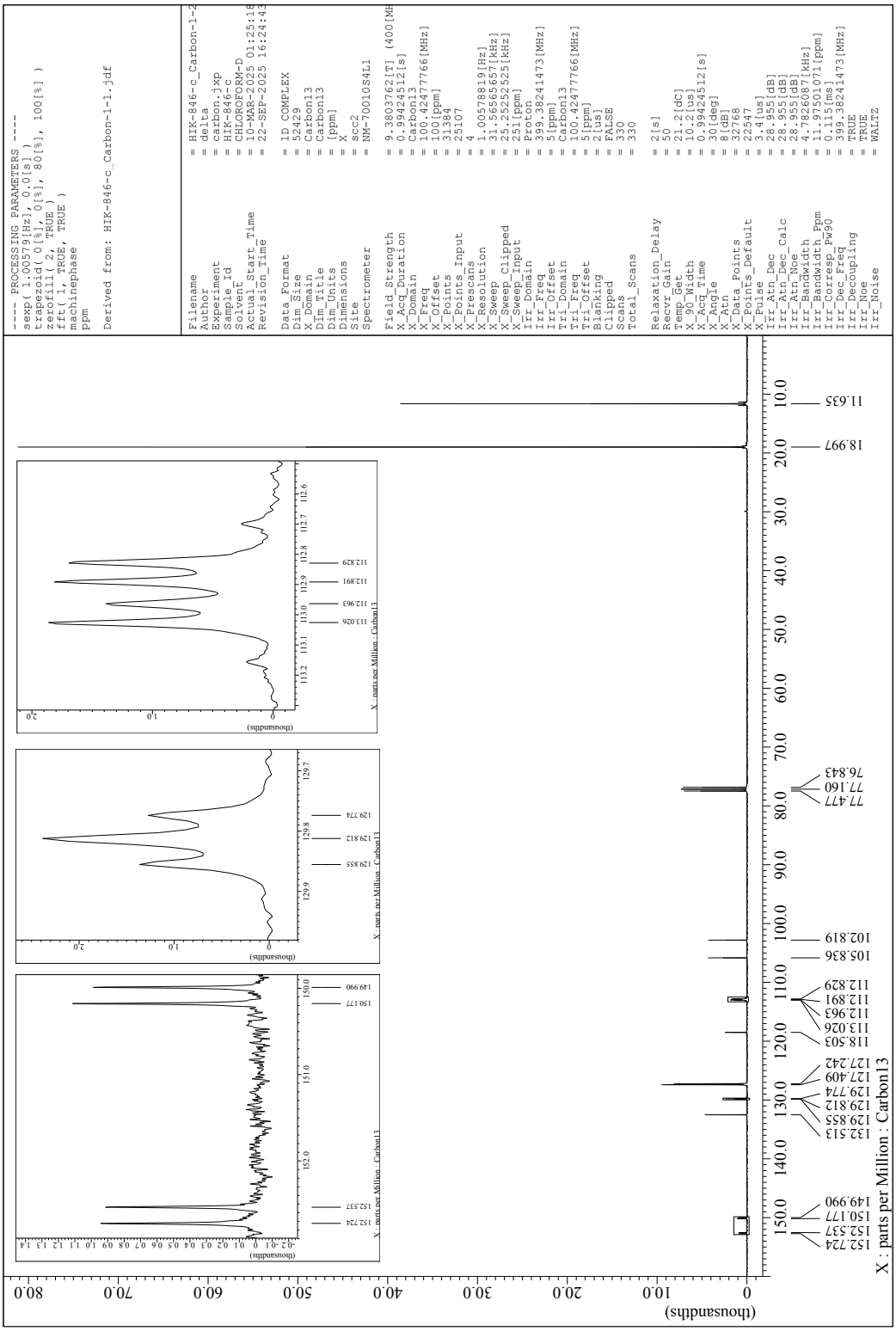

Figure S19. ^{13}C NMR spectrum (100 MHz, $CHCl_3$) of **4b**

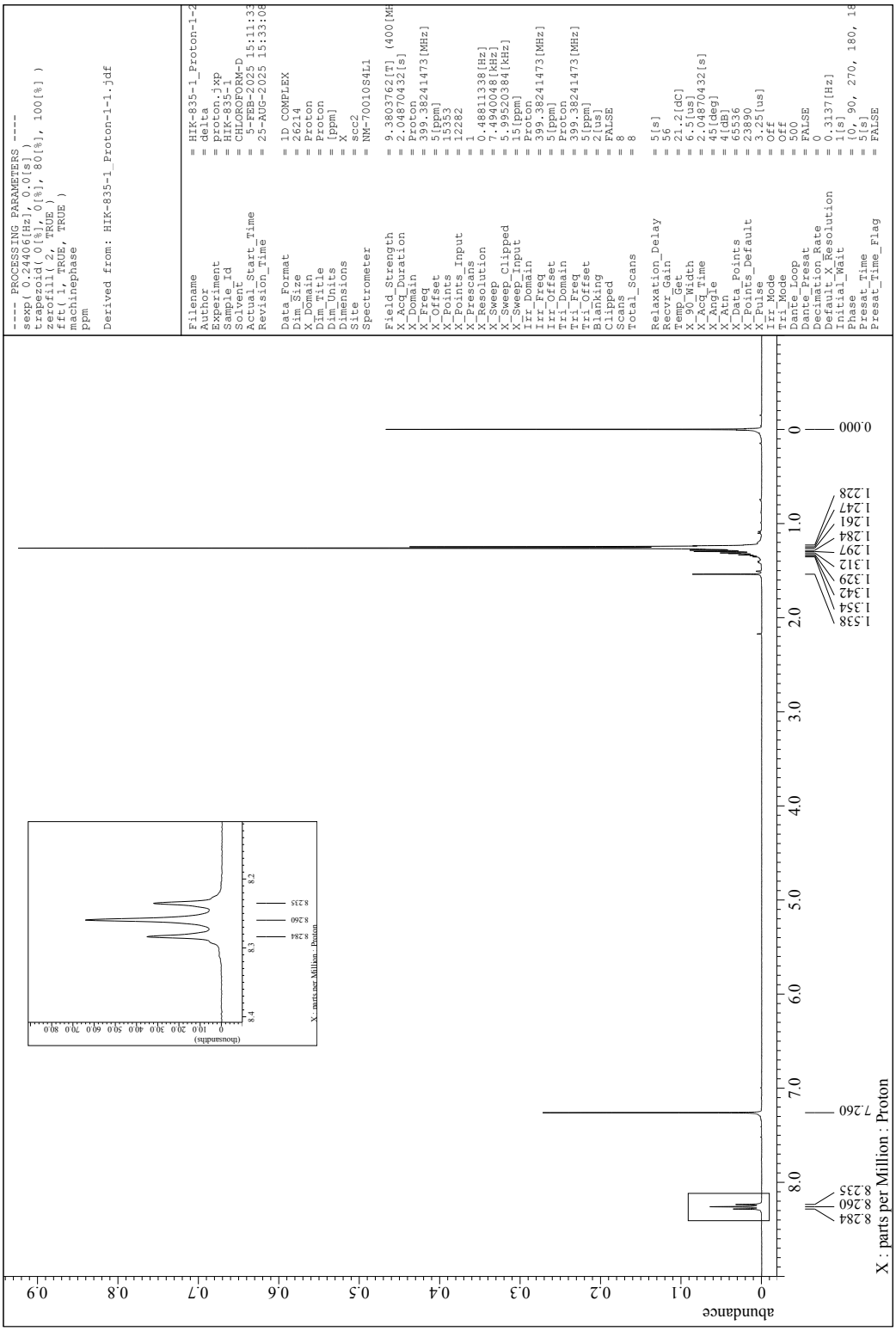

Figure S20. ^{1}H NMR spectrum (400 MHz, $CHCl_3$) of **4c**

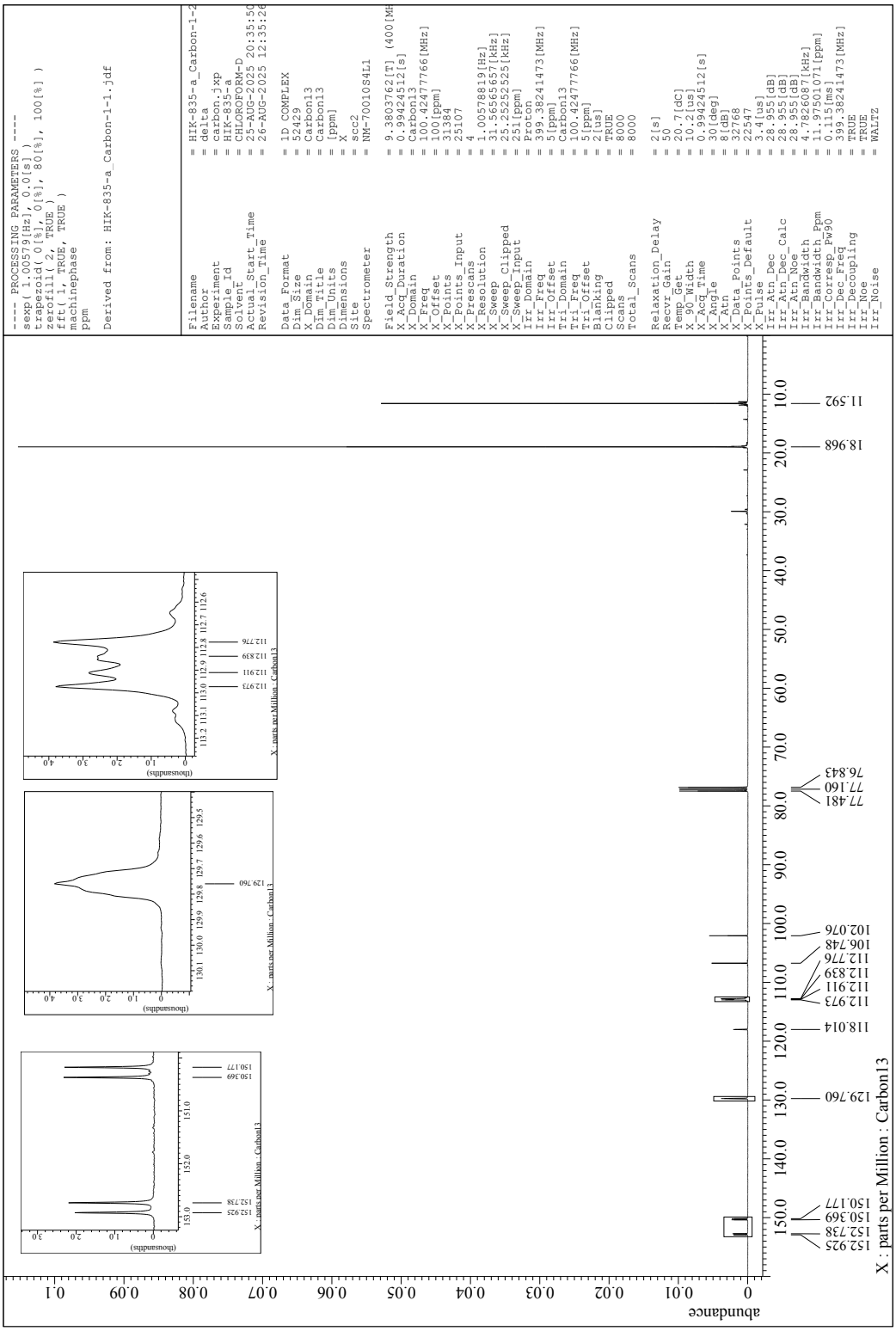

Figure S21. ^{13}C NMR spectrum (100 MHz, $CHCl_3$) of **4c**

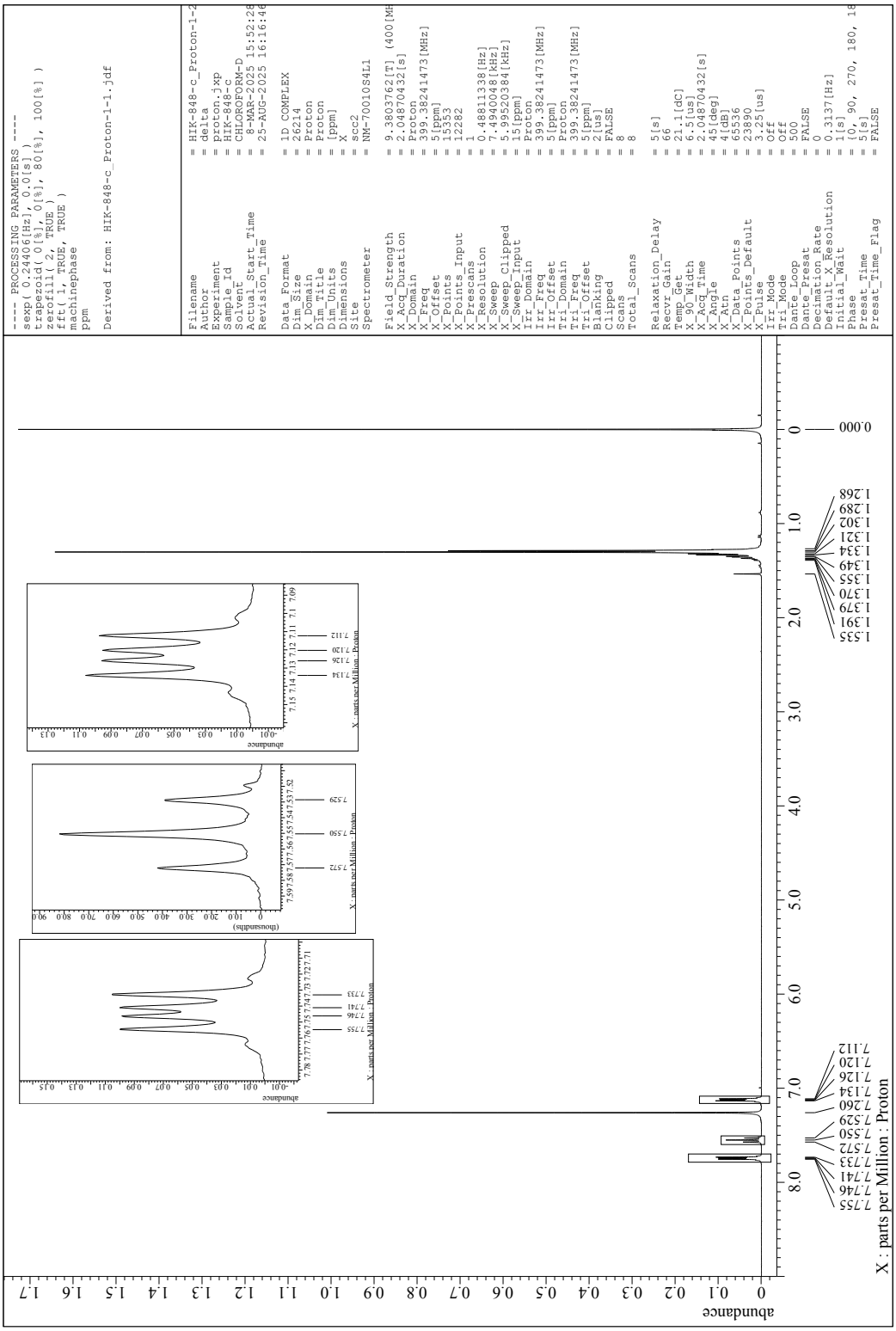

Figure S22. ^{1}H NMR spectrum (400 MHz, $CHCl_3$) of **5b**

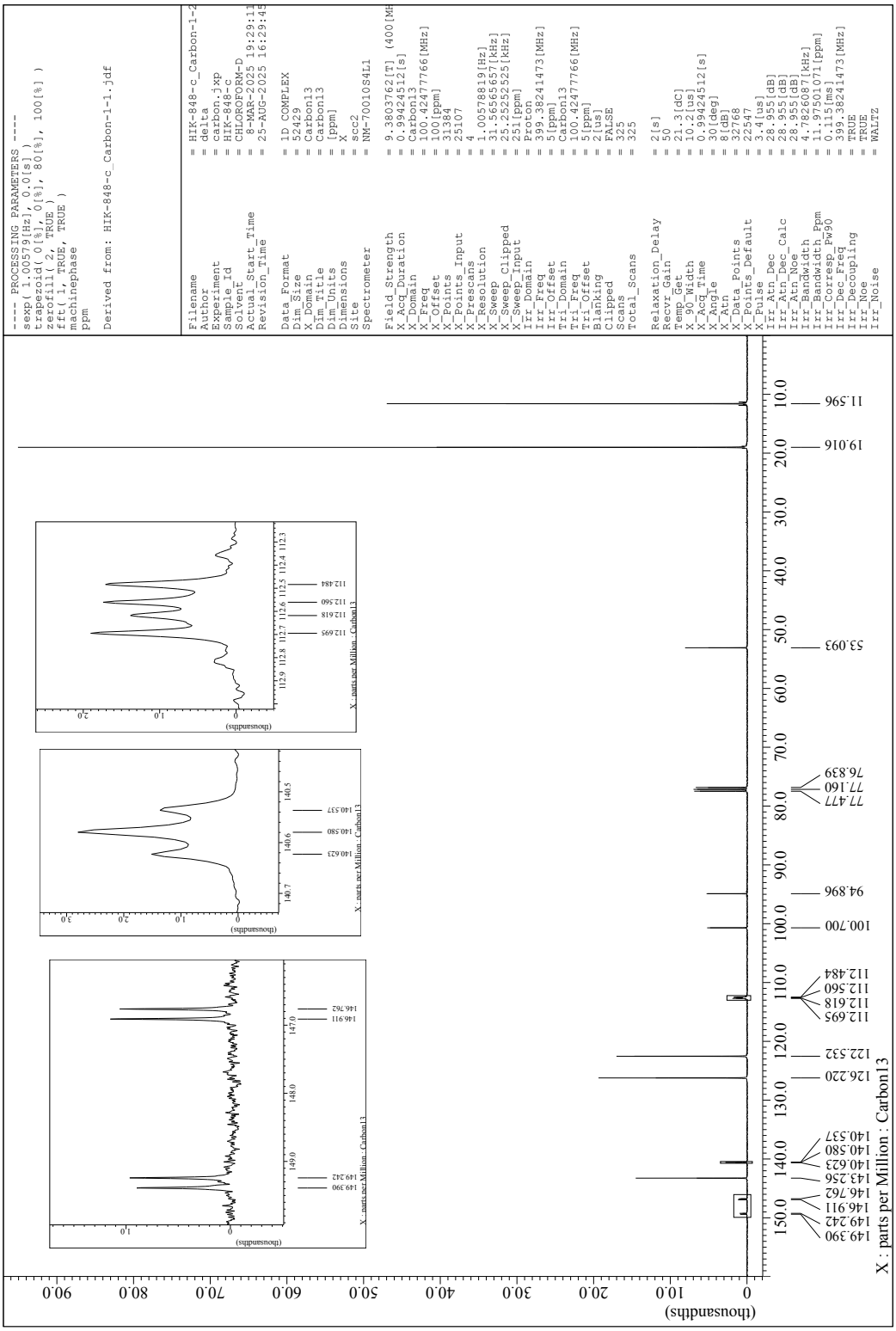

Figure S23. ^{13}C NMR spectrum (100 MHz, $CHCl_3$) of **5b**

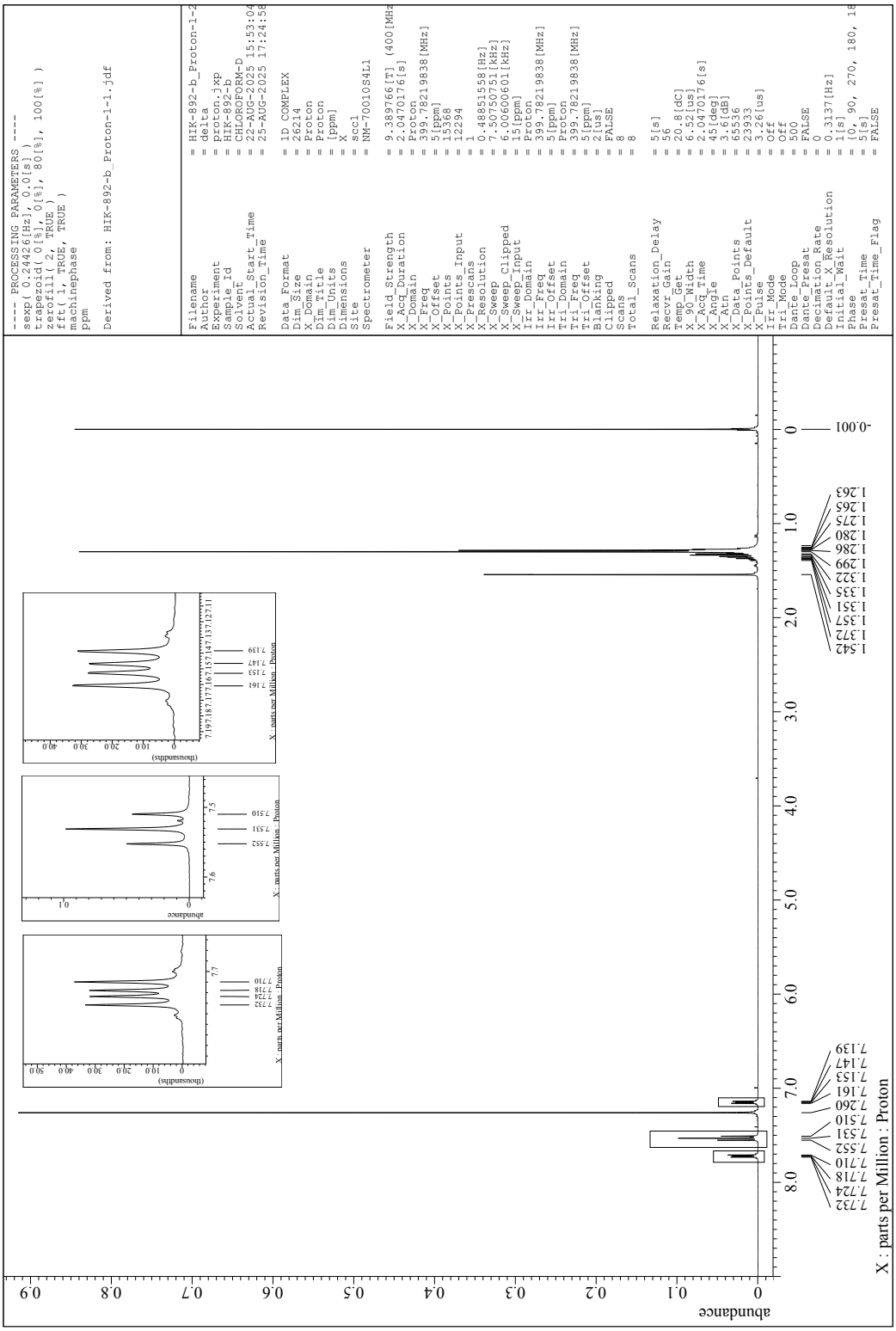

Figure S24. ^{1}H NMR spectrum (400 MHz, $CHCl_3$) of **5c**

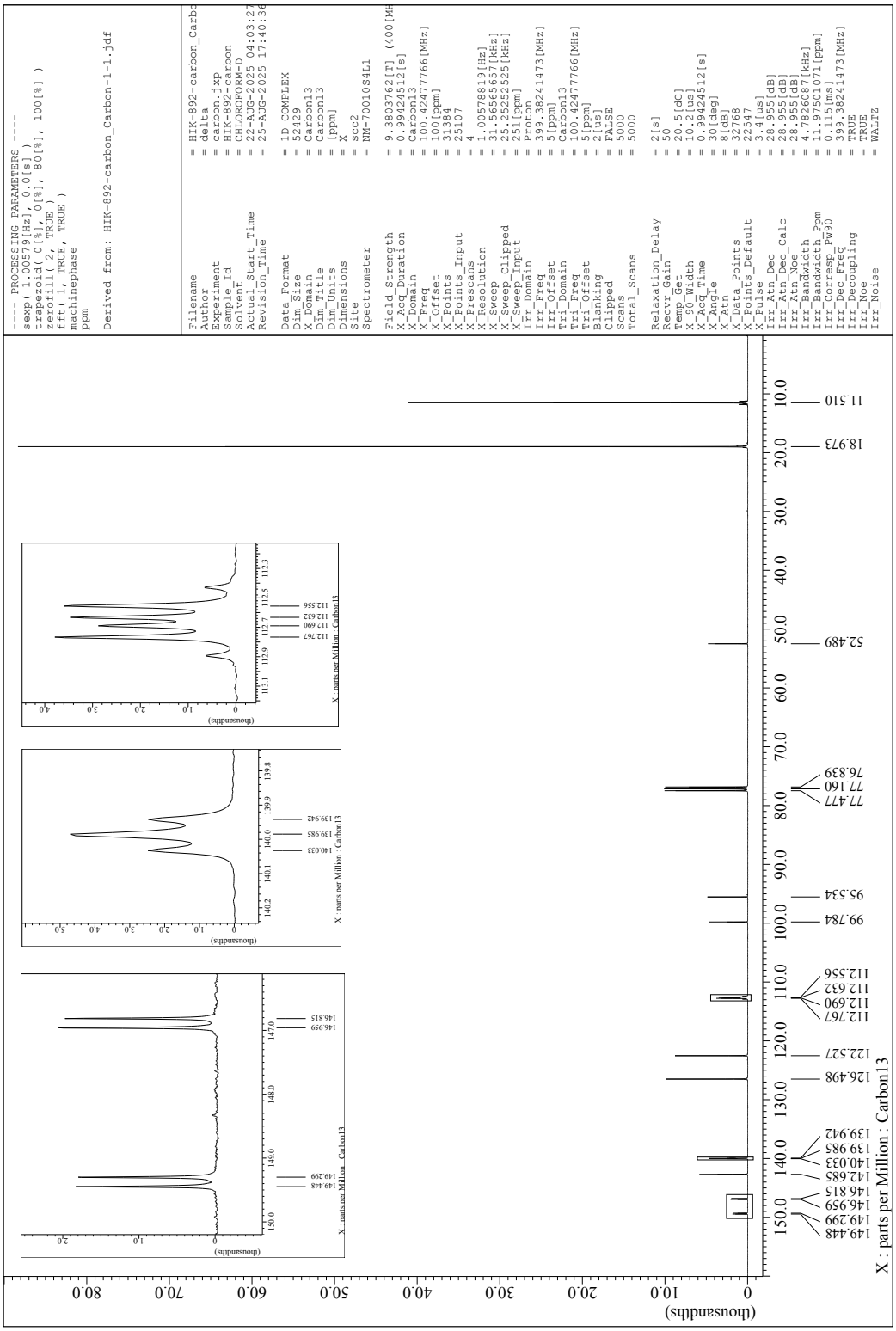

Figure S25. ^{13}C NMR spectrum (100 MHz, $CHCl_3$) of **5c**

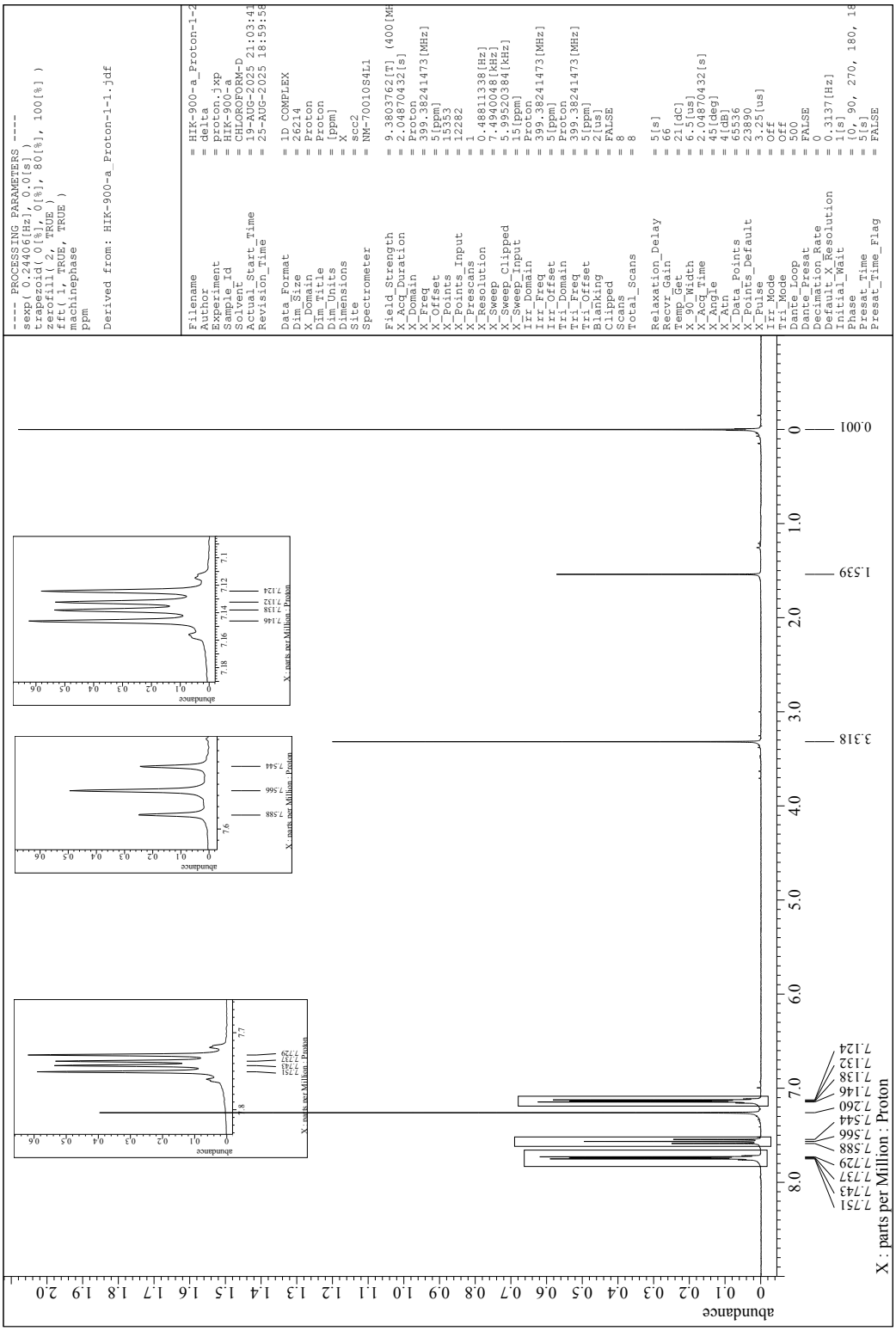

Figure S26. ^{1}H NMR spectrum (400 MHz, $CHCl_3$) of **1b**

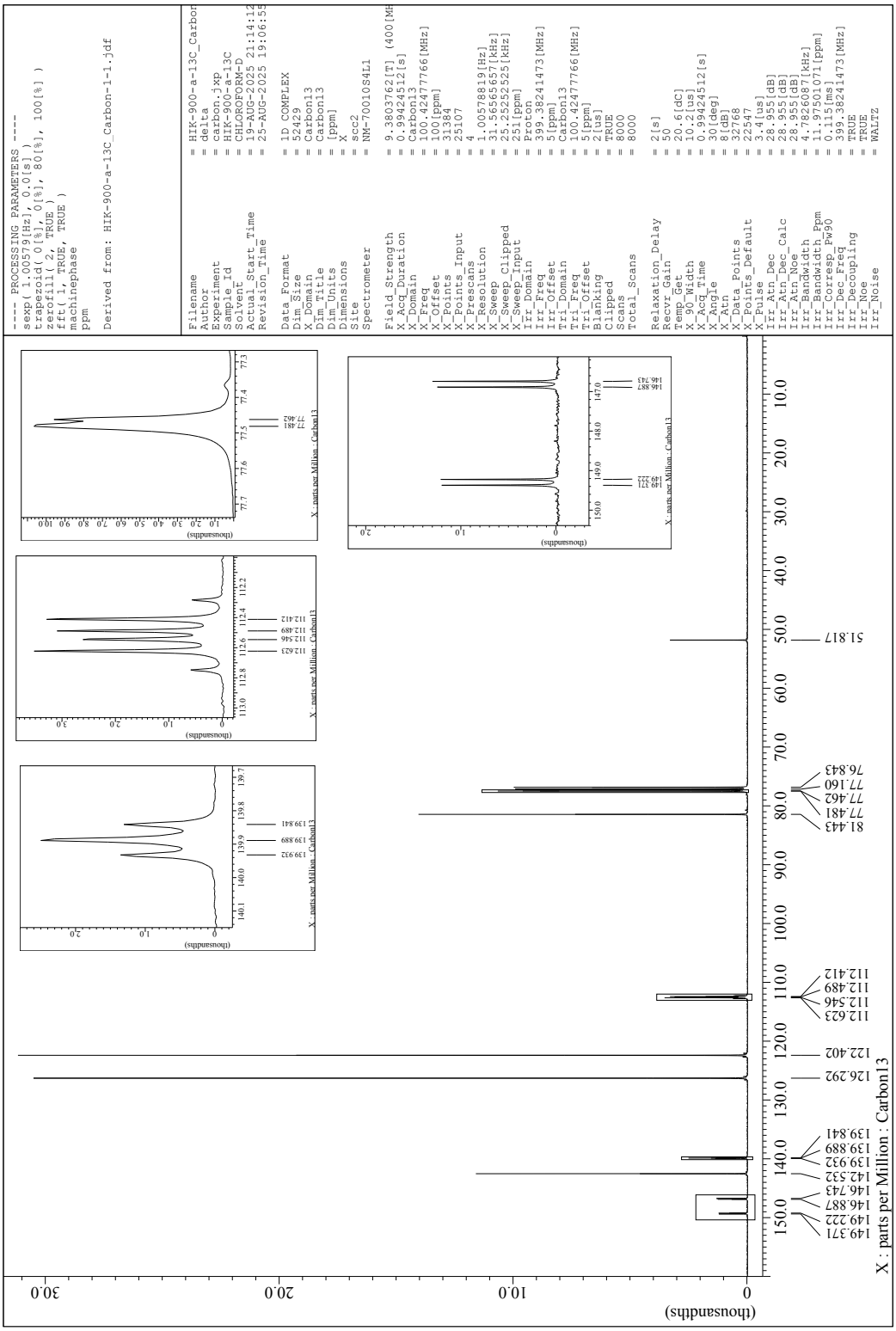

Figure S27. ^{13}C NMR spectrum (100 MHz, $CHCl_3$) of **1b**

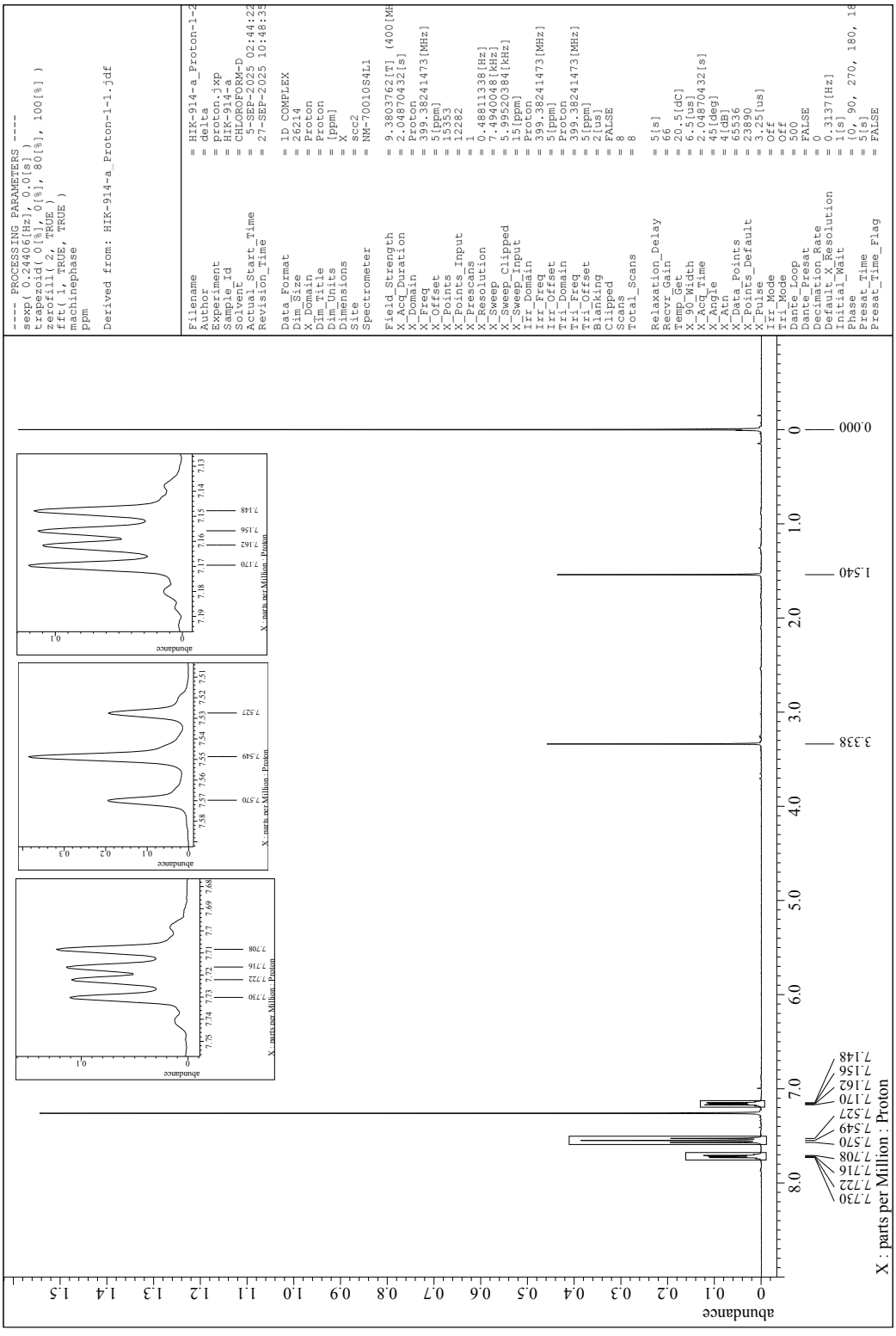

Figure S28. ^{1}H NMR spectrum (400 MHz, $CHCl_3$) of **1c**

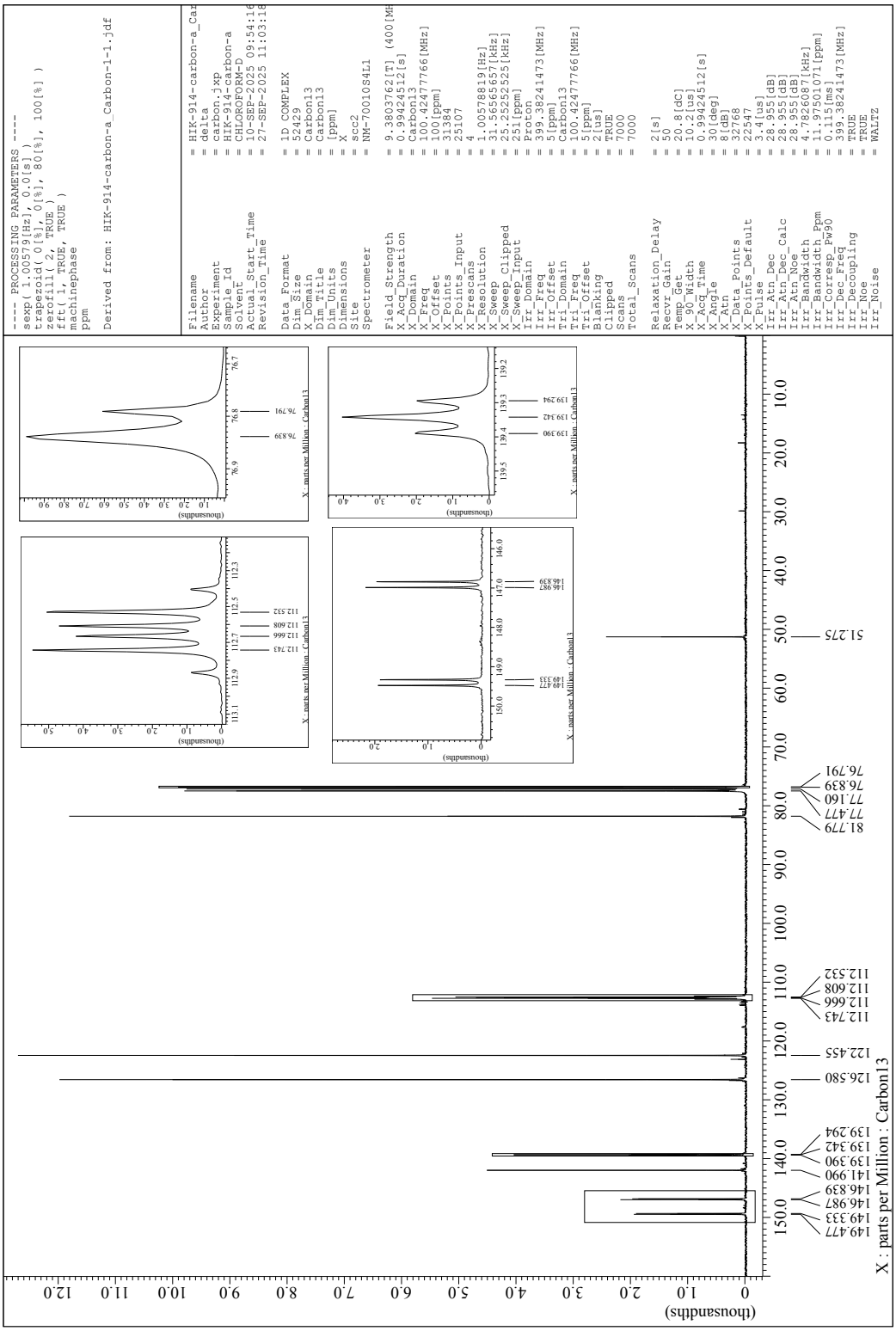

Figure S29. ^{13}C NMR spectrum (100 MHz, $CHCl_3$) of **1c**

10. Cartesian Coordinates of the Geometries used in DFT Calculations

The monomer in crystal **1a**

38

C	1.28850000	9.21980000	4.61330000
C	3.38940000	9.32760000	3.34950000
C	1.49590000	10.51690000	5.07550000
C	0.57290000	8.32140000	5.38430000
H	0.42630000	7.45440000	5.08210000
C	2.30020000	11.39560000	4.10330000
C	0.99590000	10.91650000	6.29520000
H	1.13480000	11.78420000	6.59970000
C	3.59860000	10.61250000	3.83410000
C	2.53900000	12.74580000	4.61030000
C	1.51680000	11.33540000	2.77590000
C	1.90050000	8.95660000	3.22760000
C	1.30070000	10.04100000	2.31680000
C	4.45800000	8.51480000	3.02490000
H	4.31520000	7.66080000	2.68620000
C	1.69510000	7.58300000	2.75650000
C	4.88700000	11.07470000	4.03530000
H	5.03520000	11.92750000	4.37540000
C	0.12480000	10.90450000	0.43220000
H	-0.34480000	10.76740000	-0.35850000
C	1.03580000	12.41950000	2.06470000
H	1.17690000	13.28710000	2.36800000
C	0.28300000	10.00860000	7.06390000
H	-0.05830000	10.26970000	7.88900000
C	0.60410000	9.81740000	1.14190000
H	0.45950000	8.95140000	0.83530000
C	0.07640000	8.73050000	6.61680000
H	-0.40040000	8.13020000	7.14340000
C	5.74360000	8.98880000	3.21190000
H	6.47020000	8.45150000	2.99090000
C	1.56010000	6.47060000	2.41550000
H	1.45250000	5.58740000	2.14510000
C	2.76250000	13.80540000	5.06280000
H	2.93930000	14.64520000	5.42110000
C	0.33700000	12.18330000	0.88470000

H	0.00910000	12.90280000	0.39490000
C	5.95650000	10.24720000	3.72040000
H	6.82610000	10.54760000	3.85630000

The monomer in crystal **1b**

38

C	5.12020000	10.45260000	15.04330000
C	4.93480000	11.24320000	16.17290000
C	7.08830000	10.51290000	17.05980000
C	6.97570000	12.47290000	15.63290000
F	9.00250000	8.74150000	19.51800000
C	7.26380000	9.69890000	15.93890000
C	4.03030000	9.94450000	14.35710000
H	4.15370000	9.41210000	13.60450000
C	7.16350000	11.66740000	14.51390000
C	6.24650000	11.76210000	16.78380000
C	6.59380000	10.24970000	14.67200000
F	9.34420000	7.14500000	17.38290000
C	3.66090000	11.51980000	16.62750000
H	3.53530000	12.03700000	17.39010000
C	6.05060000	12.59280000	17.97490000
C	7.66900000	10.19430000	18.27130000
H	7.54620000	10.73370000	19.01900000
C	7.43700000	13.77850000	15.65110000
H	7.30630000	14.31880000	16.39670000
C	8.02200000	8.54310000	16.02400000
H	8.13690000	7.98750000	15.28710000
C	7.81870000	12.15830000	13.40160000
H	7.94210000	11.62440000	12.65030000
C	2.74700000	10.24120000	14.80900000
H	2.00820000	9.91340000	14.34880000
C	2.56450000	11.01420000	15.92920000
H	1.70300000	11.20200000	16.22460000
C	6.76730000	9.41190000	13.49160000
C	8.43860000	9.04830000	18.33730000
C	5.90190000	13.22280000	18.95700000
H	5.78470000	13.72080000	19.73360000
C	8.60390000	8.24310000	17.24710000

C	8.09790000	14.26230000	14.53230000
H	8.41600000	15.13630000	14.52980000
C	8.29100000	13.46810000	13.42680000
H	8.74150000	13.80900000	12.68810000
C	6.86150000	8.74410000	12.52270000
H	6.93510000	8.21780000	11.75940000

The monomer in crystal **1c** ($P4_1$)

38

F	9.82050000	5.88620000	7.10250000
F	11.86490000	13.12040000	2.46910000
F	11.36180000	7.43410000	8.66070000
F	10.33830000	11.53350000	0.93880000
C	8.84530000	9.15650000	5.95950000
C	9.79370000	11.58580000	4.95940000
C	8.89090000	7.76150000	6.05540000
H	8.34790000	7.21330000	5.50160000
C	9.65420000	9.95600000	6.76020000
C	7.98820000	11.73610000	6.64130000
C	9.75480000	7.20740000	6.98740000
C	10.91380000	12.38260000	3.03780000
C	9.49320000	11.45980000	6.47060000
C	9.01030000	10.78640000	4.14910000
C	7.18460000	10.95000000	5.81380000
C	9.15390000	10.76890000	2.78460000
H	8.60050000	10.22360000	2.23810000
C	10.55830000	8.01100000	7.77560000
C	7.12700000	9.11360000	4.10880000
C	7.98950000	9.94930000	4.95550000
C	10.51540000	9.38460000	7.68070000
H	11.06530000	9.92630000	8.23450000
C	10.37190000	12.30350000	7.27800000
C	5.82580000	11.09890000	5.81380000
H	5.27930000	10.58550000	5.23090000
C	7.42740000	12.64150000	7.51100000
H	7.97000000	13.17020000	8.08420000
C	10.75550000	12.42830000	4.39650000
H	11.27950000	13.01040000	4.93560000

C	10.12500000	11.56840000	2.24090000
C	5.26100000	12.02720000	6.69500000
H	4.31820000	12.14340000	6.70980000
C	6.45490000	8.46300000	3.39450000
H	5.91260000	7.93710000	2.81750000
C	6.03370000	12.75960000	7.52440000
H	5.62250000	13.36730000	8.12820000
C	11.11770000	12.99030000	7.91370000
H	11.70900000	13.53460000	8.41950000

The unit cell in crystal **1c** ($P4_1$)

114

F	9.82050000	5.88620000	7.10250000
F	11.86490000	13.12040000	2.46910000
F	11.36180000	7.43410000	8.66070000
F	10.33830000	11.53350000	0.93880000
C	8.84530000	9.15650000	5.95950000
C	9.79370000	11.58580000	4.95940000
C	8.89090000	7.76150000	6.05540000
H	8.34790000	7.21330000	5.50160000
C	9.65420000	9.95600000	6.76020000
C	7.98820000	11.73610000	6.64130000
C	9.75480000	7.20740000	6.98740000
C	10.91380000	12.38260000	3.03780000
C	9.49320000	11.45980000	6.47060000
C	9.01030000	10.78640000	4.14910000
C	7.18460000	10.95000000	5.81380000
C	9.15390000	10.76890000	2.78460000
H	8.60050000	10.22360000	2.23810000
C	10.55830000	8.01100000	7.77560000
C	7.12700000	9.11360000	4.10880000
C	7.98950000	9.94930000	4.95550000
C	10.51540000	9.38460000	7.68070000
H	11.06530000	9.92630000	8.23450000
C	10.37190000	12.30350000	7.27800000
C	5.82580000	11.09890000	5.81380000
H	5.27930000	10.58550000	5.23090000
C	7.42740000	12.64150000	7.51100000

H	7.97000000	13.17020000	8.08420000
C	10.75550000	12.42830000	4.39650000
H	11.27950000	13.01040000	4.93560000
C	10.12500000	11.56840000	2.24090000
C	5.26100000	12.02720000	6.69500000
H	4.31820000	12.14340000	6.70980000
C	6.45490000	8.46300000	3.39450000
H	5.91260000	7.93710000	2.81750000
C	6.03370000	12.75960000	7.52440000
H	5.62250000	13.36730000	8.12820000
C	11.11770000	12.99030000	7.91370000
H	11.70900000	13.53460000	8.41950000